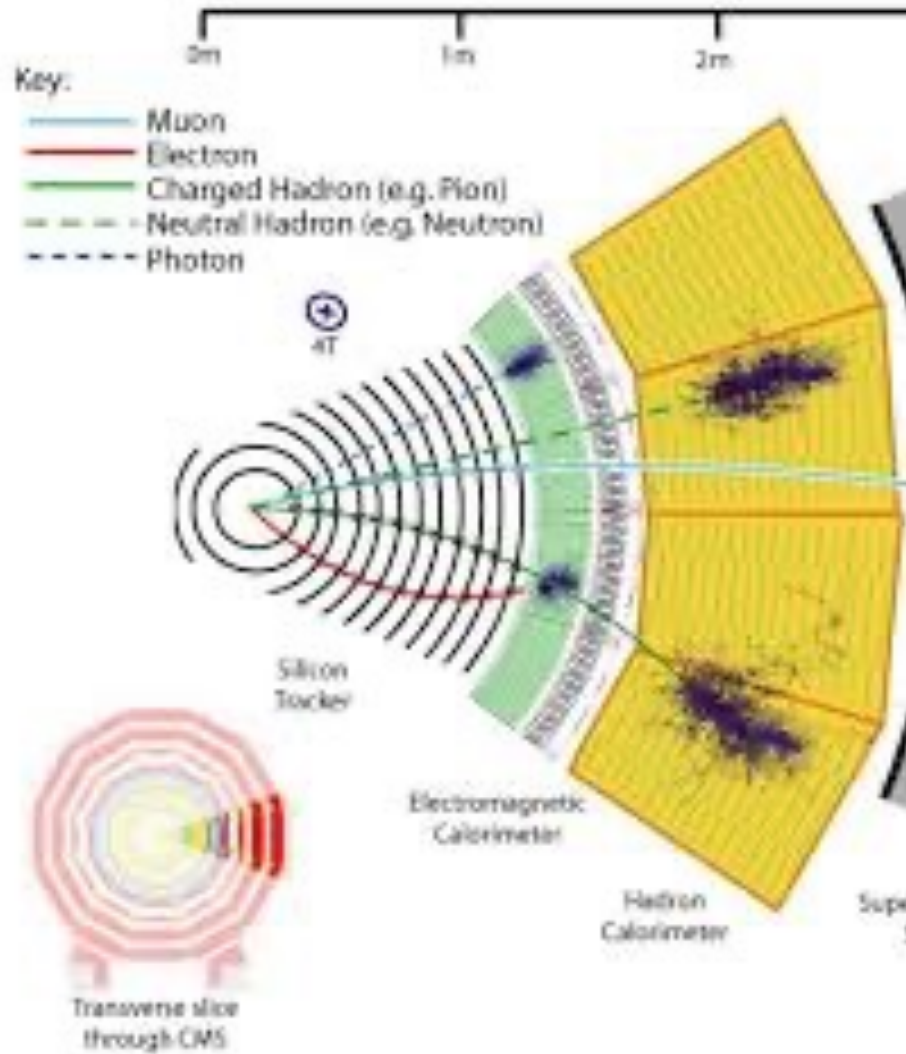


Instrumentation for Particle Physics – in two lectures

Lecture B: Tracking, Calorimetry, Particle Identification, Muon Detection, Neutrino Detection, and the Future



Sally Seidel
University of New Mexico

African School of Physics 2024

Tracking Detectors:
Measure particle trajectory (curvature, momentum)
and point of origin (“vertex”)

Note: these lectures will not cover historical detector designs that are no longer in use.

The “ancestor” – and still in use: **Wire chambers**

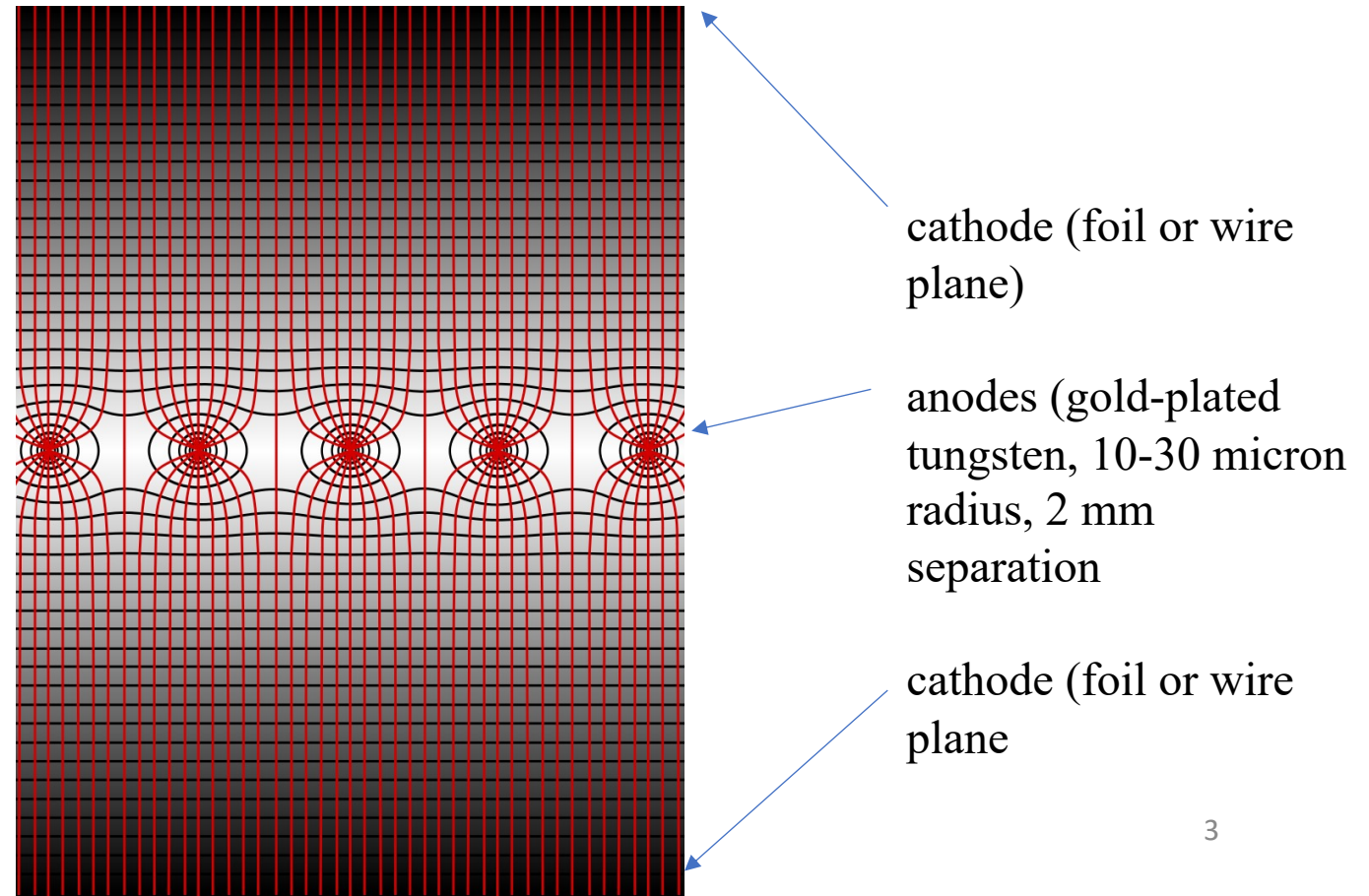
The single wire proportional counter: invented* by Geiger and Rutherford in 1908.

Multiwire proportional chambers (MWPC) were invented** by Georges Charpak in 1968 (Nobel Prize 1992)

MWPC: A planar layer of proportional counters without separating walls

produces field lines (red) and equipotential lines (black) like this:

- A through-going charged particle ionizes gas, produces primary electrons and ions along the track
- Primary electron drifting toward anode is accelerated by the E field, starts avalanche (ions + more electrons)
- Avalanche multiplication ends when positive ion space charge reduces E field below critical value
- Electron cloud drifts toward anode, ion cloud drifts (more slowly) to cathode.



* H. Geiger and E. Rutherford, Proc. Royal Soc. A 81:141 (1908).

** G. Charpak et al., Nucl. Instr. Meth. A 62: 262 (1969).

MWPC design considerations:

Position resolution σ , in the direction perpendicular to the wires, for wire separation d :

$$\sigma = \frac{d}{\sqrt{12}} = 580 \text{ microns} \quad (\text{for } d = 2 \text{ mm})$$

The wire separation is limited by ***electrostatic repulsion*** of the long anodes. Counterbalance this with ***wire tension***.

For anode voltage V , length ℓ , capacitance per length C , tension T , permittivity ϵ_0 , ***the requirement for stability*** is:

$$T \geq \left(\frac{V \ell C}{d} \right)^2 \cdot \frac{1}{4\pi\epsilon_0}$$

Capacitance depends on anode separation d , anode wire radius r , and perpendicular distance L from anode to cathode:

$$C = \frac{4\pi\epsilon_0}{2 \left(\frac{\pi L}{d} - \ln \frac{2\pi r}{d} \right)}$$

An anode wire of mass m ***sags under gravity*** (this reduces the homogeneity of the E field) by an amount:

$$f = \frac{m\ell g}{8T}$$

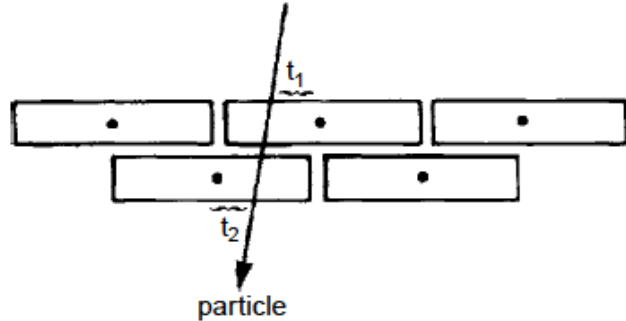
To improve spatial resolution in the direction along the wire:

-segment the cathode, then measure the charge induced on the cathode and calculate the center of gravity of the induced charge

- Resolution ~ 50 microns is typical for tracks perpendicular to the wire plane.

Using timing to improve the spatial resolution: **the drift chamber***

- Introduce potential wires between the anodes, to shape the drift field, *seeking well-mapped drift velocity v* .
- *Measure the time t* between particle traversal of chamber and electron cloud arrival at anode.



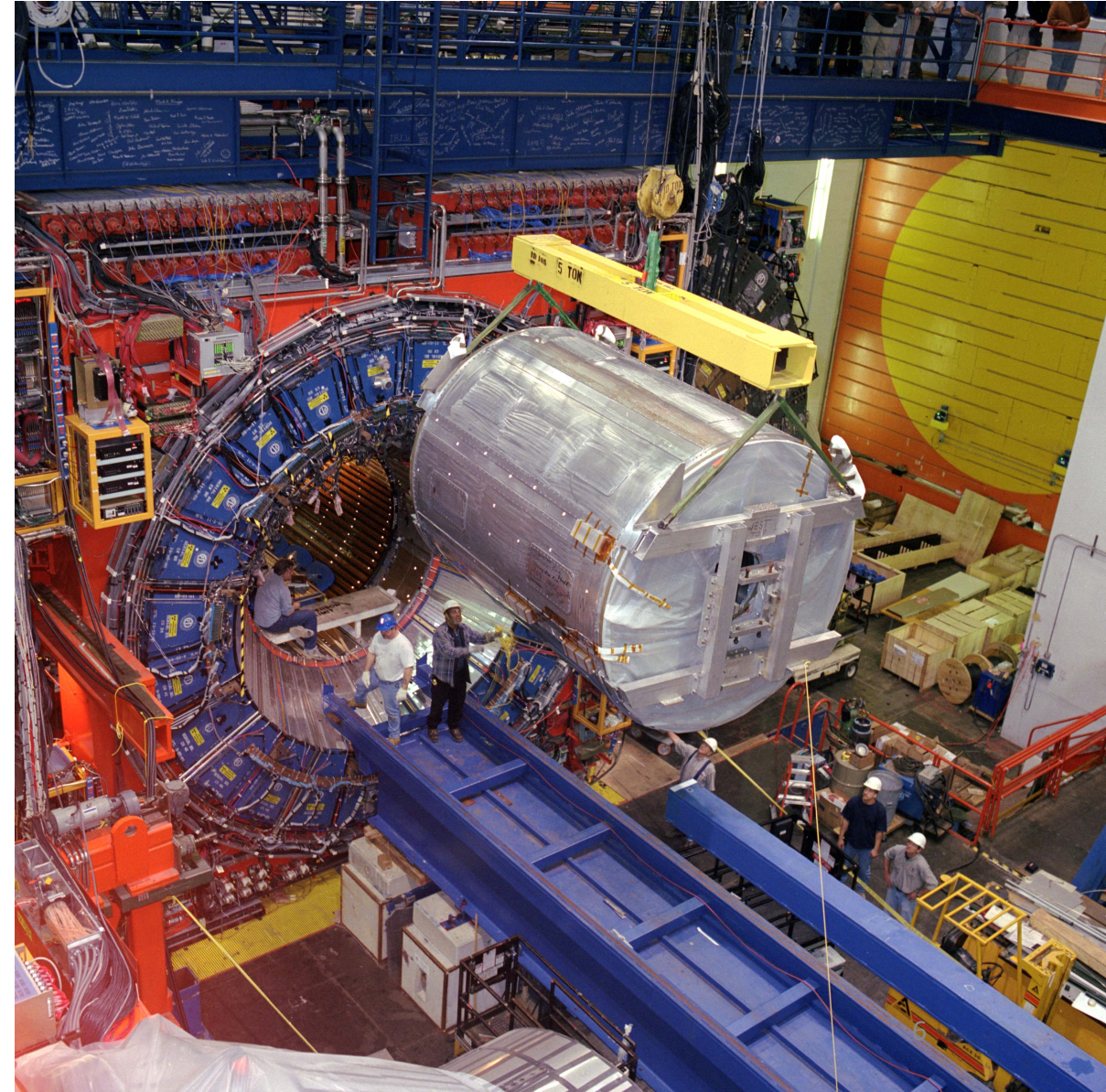
- *Perpendicular distance x from track to anode* is then

$$x = \int v^-(t) dt$$

- For electronic time resolution $\sim 1\text{ns}$, in smallish chambers not limited by mechanical tolerances, *spatial resolution on $\sigma_x \sim 20\mu\text{m}$* (ignoring fluctuations in formation of the primary ionization, and diffusion of the cloud).

* A.H. Walenta et al., Nucl. Instr. Meth. A 92: 373 (1971).

Drift chambers can be big!
**Installation of the the CDF Central
Outer Tracker (drift chamber):**



Varieties of modern wire chambers

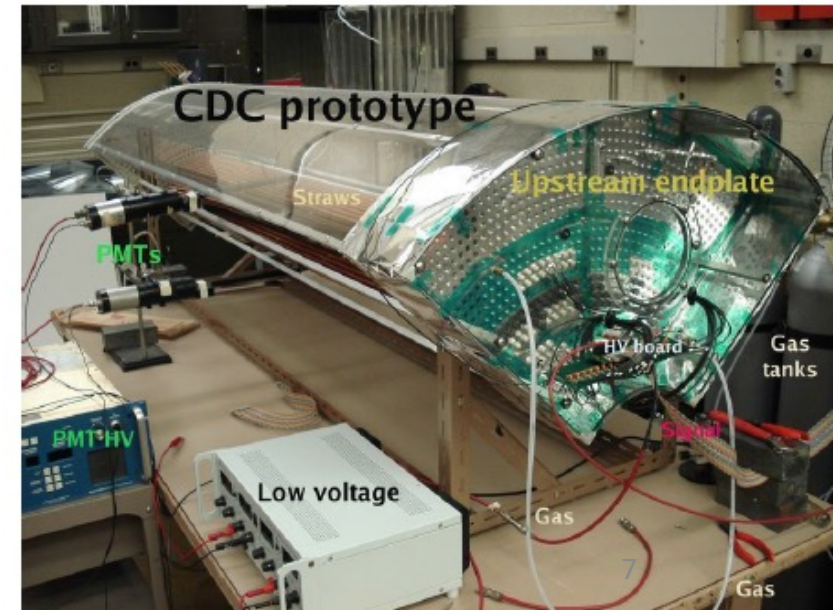
1) *Cylindrical proportional and drift chambers*

- Wires run axially, form cylindrical volumes
- Wires are stretched between 2 end plates, for total tension of tons
- Embed the chamber in an axial magnetic (B) field.
- Potential wire between each pair of anodes.
- Then these record track curvature to infer momentum p. For radius of curvature ρ ,

$$p[\text{GeV} / c] = 0.3B[\text{T}] \cdot \rho[\text{m}]$$

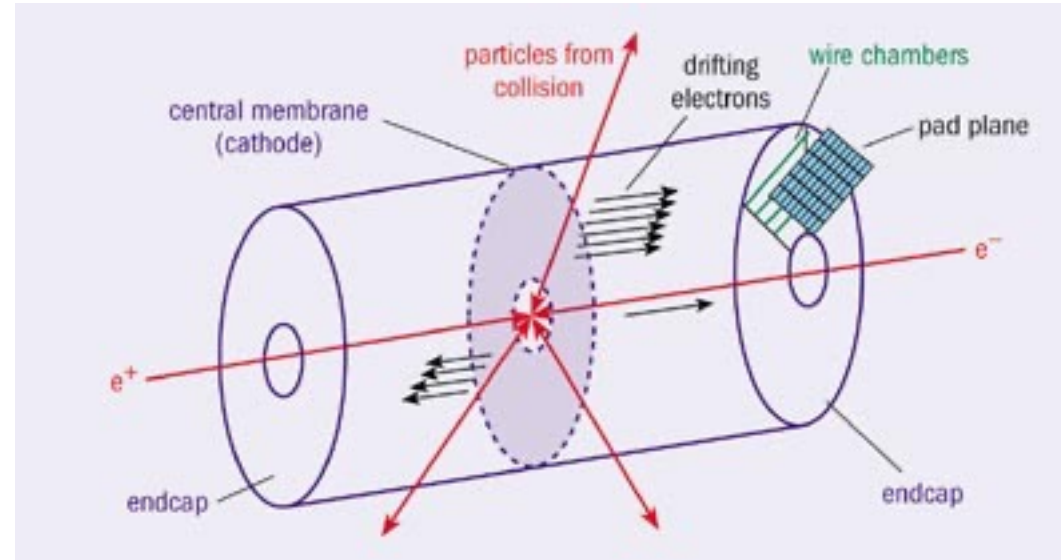
- To obtain axial position information: half of the anode wires are oriented at a small *stereo angle* ($\sim 2^\circ$) with respect to the z-axis.
- Drift cells can be “*open*” or “*closed*” depending on whether or not there is a field wire between every pair of anodes. Closed: shapes the field better, but costs more wires.
- *If a wire breaks* – a region of the chamber is disabled. To minimize this effect, *surround each wire with a mylar foil (this is a “straw tube”)* and the full assembly is a “straw chamber”

$\frac{1}{4}$ prototype of the
GlueX straw
chamber



2) *Time projection chambers** (David Nygren, 1974) measure a 3-dimensional space point for every cluster of primary electrons, with *minimal multiple scattering*

- one central electrode
- E and B fields both axial (no $\mathbf{E} \times \mathbf{B}$ effect): charge drifts parallel to field lines.
- volume contains counting medium (gas or liquid) but no other components: minimal multiple scattering
- end plates are wire chambers



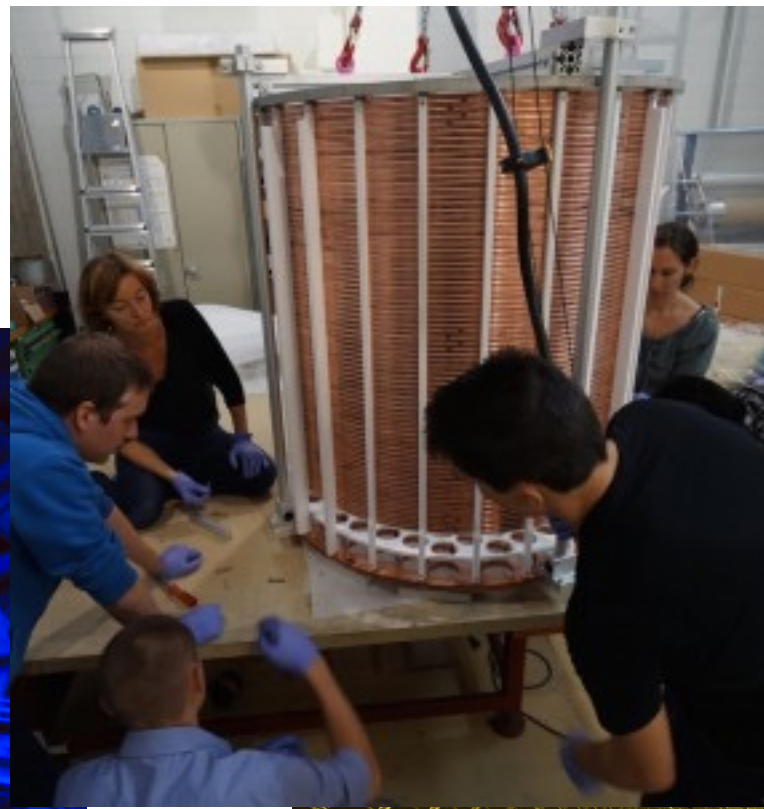
- Axial B field: suppresses perpendicular diffusion (charged particles spiral around the field lines)
- Arrival time of charge – determines the z coordinate of the event
- Anode wires in the endcaps – stretched in the azimuthal direction to measure radius r
- Cathode pads around the circumference of the end plates: to measure angle ϕ and radius r
- Analog signals on the anodes measure energy loss: particle ID

* D. Nygren et al., PEP-PROPOSAL-004, App. A6 (1976).⁸

Modern TPC's: can achieve very large volume. Detection rate is limited by drift + analog readout times; no amplification in noble liquids.

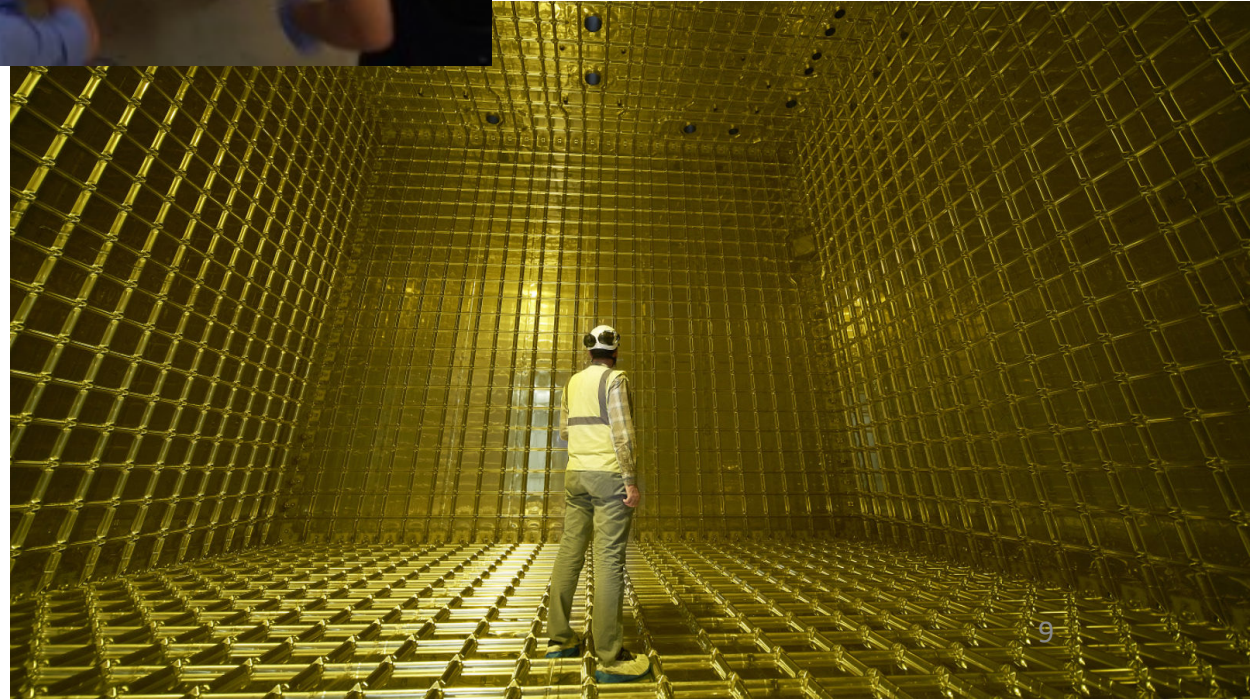


ALICE at CERN uses Ne-CO₂ gas



XENON dark matter experiment at Gran Sasso uses 62 kg dual phase (liquid/gas) Xe

Support structure for the liquid argon TPC (LArTPC) in DUNE



Improve resolution by *miniaturizing the ionization volume*: **Micro-pattern Gas Detectors**

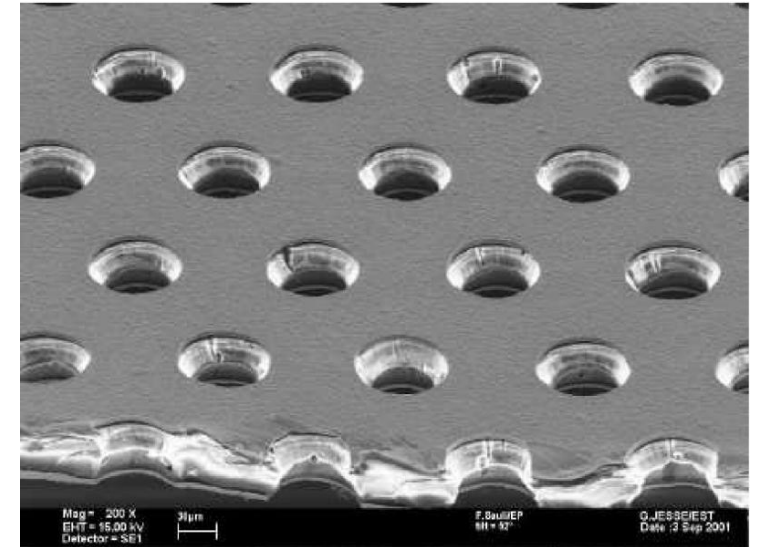
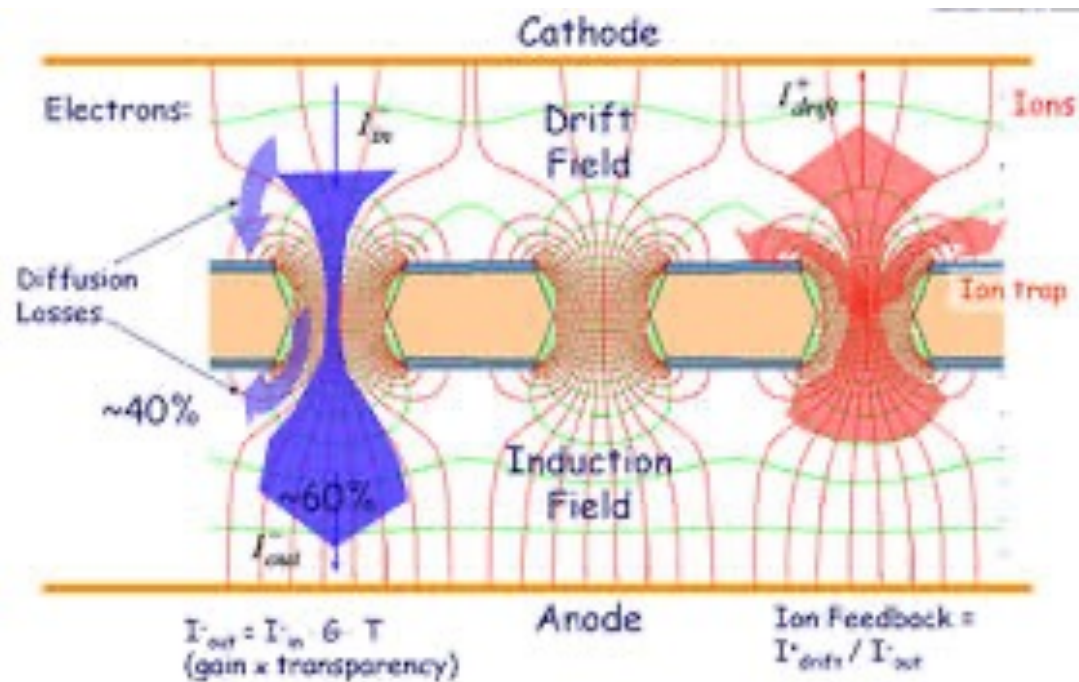
- These are MWPC's miniaturized (by ~factor of 10), with gas gaps of $\sim 2 - 10$ mm.
- *Electrodes are formed by lithography on insulator or semiconductor surfaces* (i.e., no wires). Pitch $\sim 100 - 200$ microns.
- Strips or pixels
- *Low dead time* (ion drift distance to cathode is short).
- Many varieties, to *optimize against aging and for different conditions*.
- Examples (these both include an amplification structure): **Micromegas** and **GEM**

Improvement in rate capability: capable of $\sim 10^6$ Hz/mm²

Improvement in granularity: capable of ~ 30 μ m spatial resolution

Gas electron multiplier (GEM)*

Also include *a conversion gap*, plus *a multiplication region* produced by a thin insulating Kapton foil coated with metal film on both sides, and containing $\sim 50 \mu\text{m}$ holes on a $\sim 100 \mu\text{m}$ pitch. Different potentials on the films produce charge multiplication in the holes. *Gain* $\sim 10^5$ on electrons for cascaded arrays. Short gap restricts breakdown.



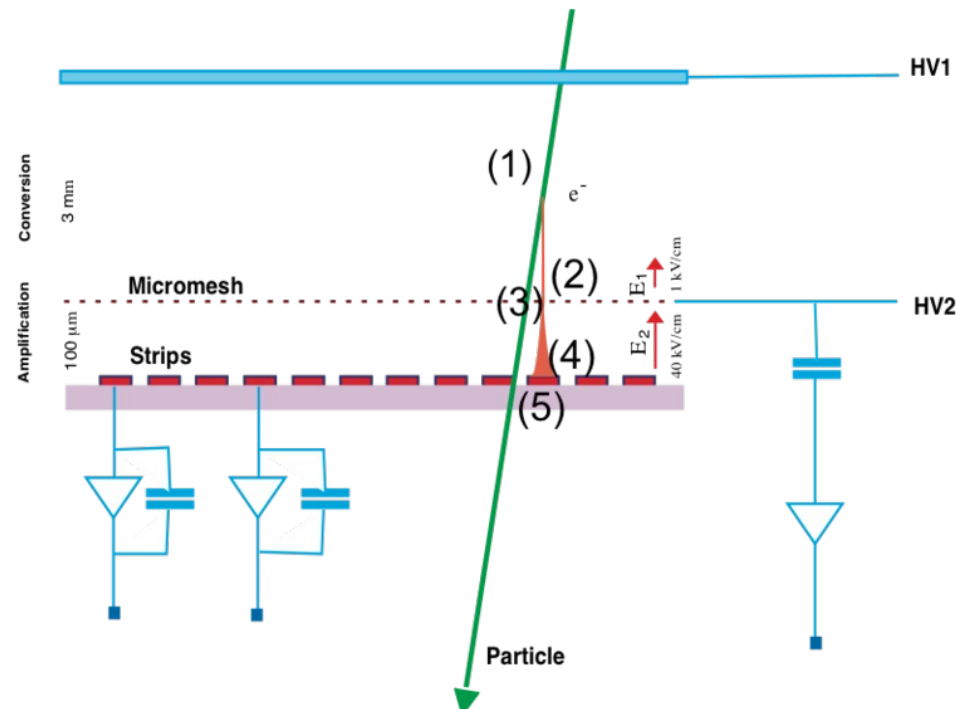
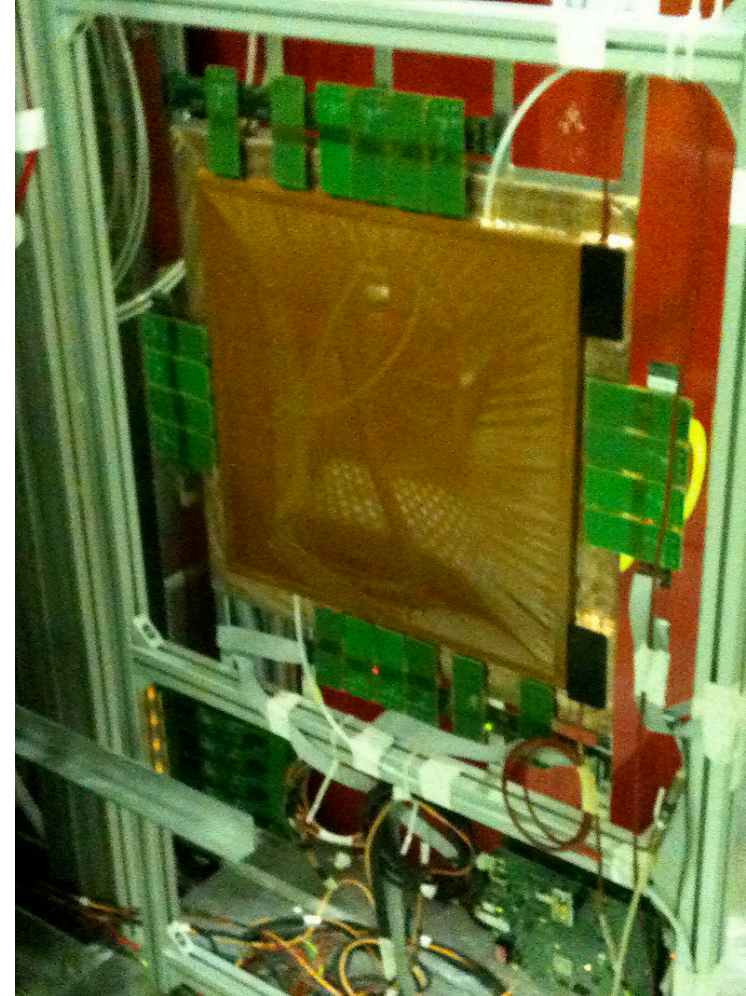
GEM technology is also proposed for the ILC TPC.

* F. Sauli, Nucl. Instr. Meth. A A 386: 531 (1997)

Micro-Mesh Gas Structure (Micromegas)*

- Primary electrons are produced in the ionization process in a **2-5mm conversion gap**, then drift to a **50-100 μm multiplication gap**, bordered by a cathode mesh and anode readout structure.
- High E field (~ 100 kV/cm) in the multiplication gap provides **gain $\sim 10^5$** on electrons.
- Ions are collected in the near cathode, so **timing precision and rate capability are good**.

Micromegas is operating in the COMPASS Experiment...



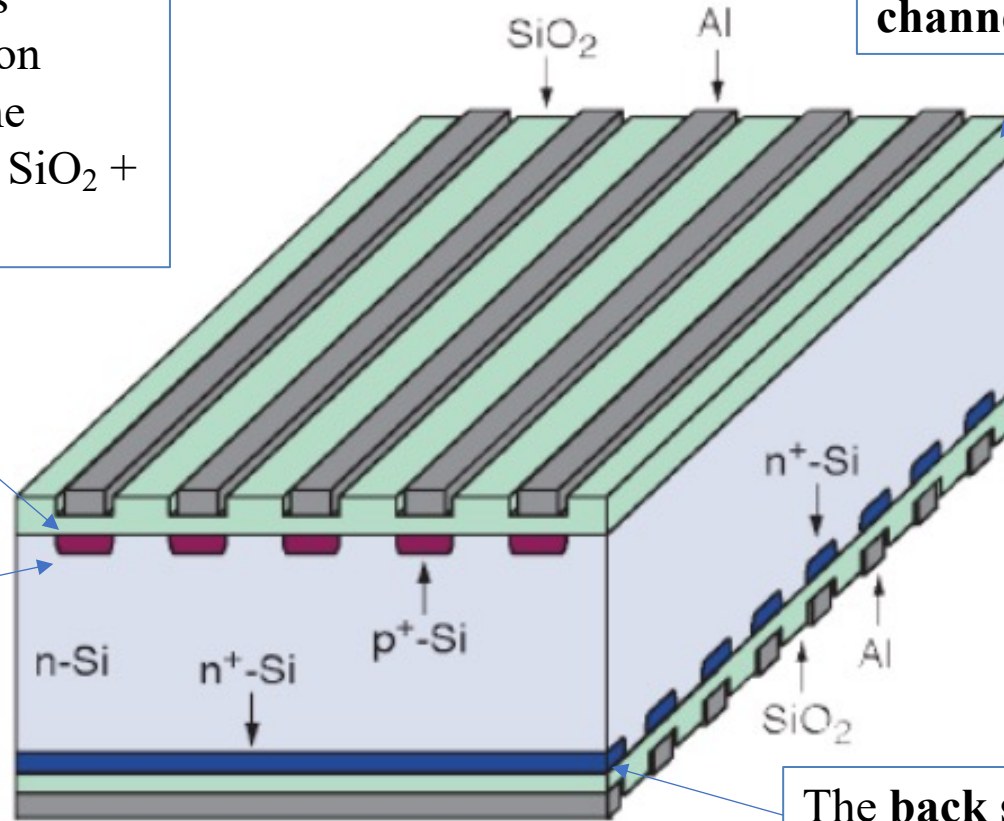
...and has been proposed for a “Micromegas TPC” at the International Linear Collider (ILC)

* Y. Giomataris et al., Nucl. Instr. and Meth. A 376: 29 (1996).

Silicon Pixel and Strip Detectors: replace the ionization medium (gas) with semiconductor, for the ultimate precision

In modern detectors, typically signal routed to read-out electronics is capacitively induced on **metal electrodes**. The capacitor dielectric is $\text{SiO}_2 + \text{Si}_3\text{N}_4$.

SiO_2 grows naturally on wafer surface, and electrically **isolates channels**.



The pn junction is at the interface of the bulk with these **implanted strips** (“p⁺” means $10^{18} \geq n_{\text{dopant}}/\text{cm}^3 \gg 10^{13}$). Under *reverse bias*, the region depleted of free carriers grows from the junction toward the n⁺ side (“back side”).

The **back side also takes an implant**, which can be segmented (in “double sided detectors”) or not.

Calorimetry: Measurement of Energy,
Missing Energy, and Particle ID

Calorimetric method: *total absorption of the energy* of a particle, in material bulk, then measurement of the deposited energy. The particle is destroyed in the process.

Applies to *neutral and charged* particles.

Role of the calorimeter:

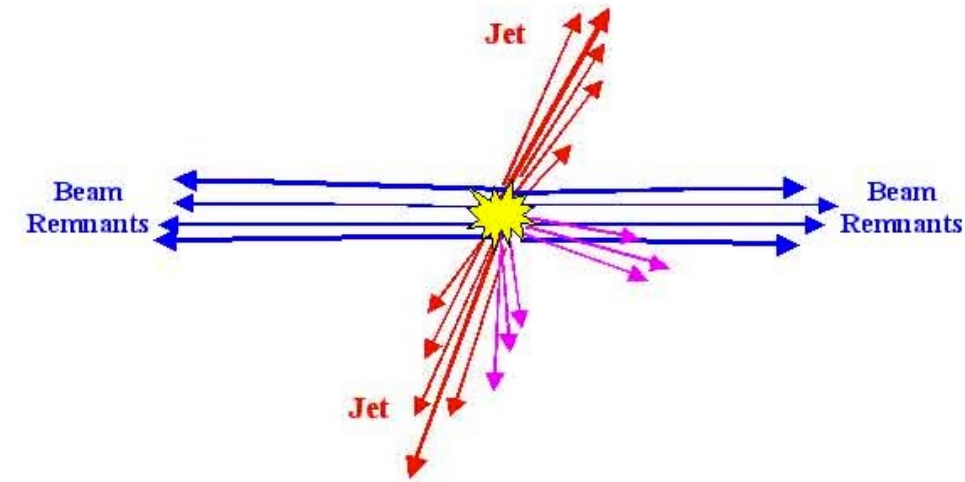
- precision measurement of the four-vectors of individual particles and jets
- measurement of mass peaks
- measurement of energy flow, to recognize missing energy
- identification of jet substructure
- rejection of pileup (multiple overlapping interactions during a single beam crossing)

Measurement principles use

- atomic and molecular excitation (ionization, scintillation)
- collective effects in the medium (Cherenkov light, phonons)
- heat deposition (transition from superconducting to normal)

In addition to measuring energy, *the calorimeter can provide full information on the track 4-vector as well as fast input to a detector trigger.*

Very different physics for detection of electromagnetically showering particles (electrons, positrons, photons) **versus strongly interacting (i.e. hadronic) particles** (pions, kaons, protons, neutrons)



Electromagnetic calorimetry

Principle of detection: Energy loss (dE/dx). Here is what dominates the process:

- for showering particles with energy \sim MeV
 - for photons - photoelectric and Compton
 - for charged particles – ionization and excitation

} These do not produce a shower / avalanche
- for showering particles with energy \gtrsim 100 MeV
 - for photons – pair production
 - for charged particles – bremsstrahlung

} These DO produce a shower / avalanche

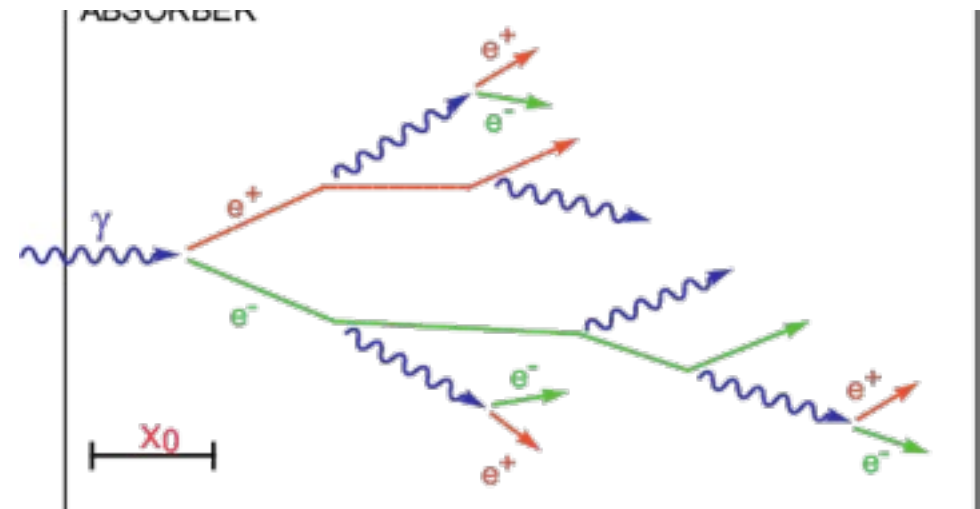
Recall that **radiation length X_0** characterizes the loss rate:

$$-\frac{dE}{dx} = \frac{E}{X_0}$$

Think of X_0 as “the typical distance the electron travels before it brems, or the typical distance the photon travels before it converts to a pair.”

Typically the **depth t** of an EM calorimeter is indicated in units of radiation lengths:

$$t = \frac{x}{X_0}$$



In a simplified model of the shower, *the # shower particles at depth t* is:

$$N(t) = 2^t$$

If the primary incident particle has energy E_0 , the *energy of each particle in generation t* is:

$$E(t) = E_0 2^{-t}$$

The *shower stops when*

$$E_0 / N < E_c$$

where E_c is a critical energy at which Compton/photoelectric/ionization begin to dominate (depends on the material).

Thus:

$$E_c = E_0 2^{-t_{\max}}$$

And the *position of the shower maximum* is

$$t_{\max} = \frac{\ln(E_0 / E_c)}{\ln 2}$$

Thus: in designing, **the thickness of the calorimeter should go as $\ln E_0$.**

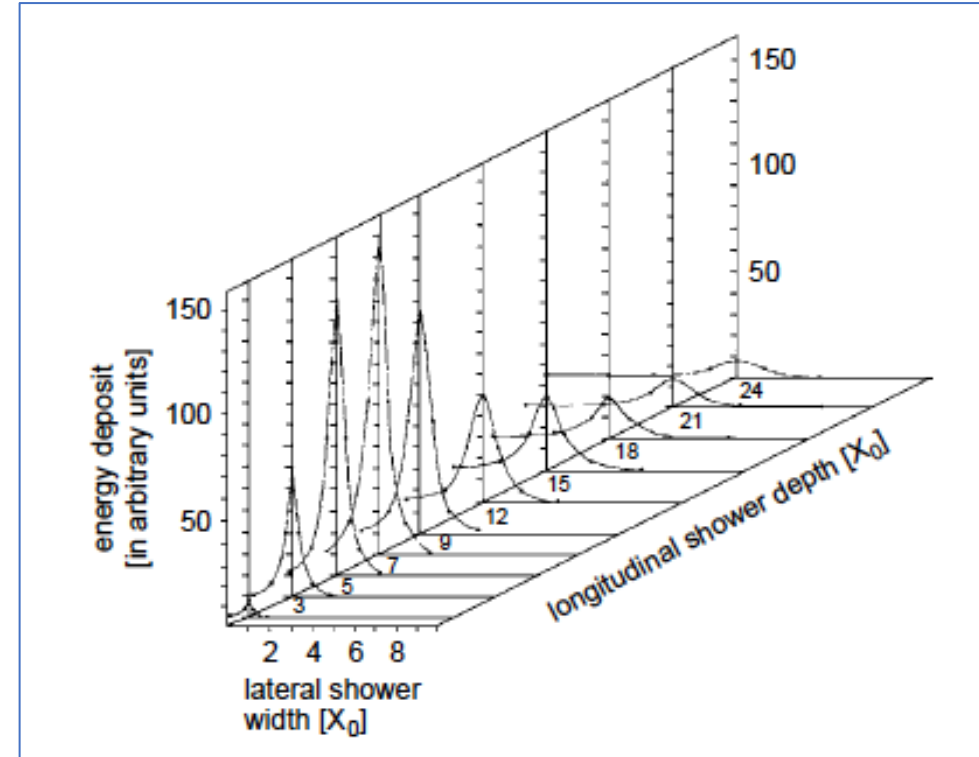
Note: below E_c , production of electrons and positrons stops within $1 X_0$, but photons continue to penetrate a further 7-9 X_0 . **To fully contain a shower, the calorimeter should have depth $\sim 16 X_0$.**

The actual formation of the shower is more complicated than this but can be well modeled using Monte Carlo, as:

$$\frac{dE}{dt} = E_0 \cdot b \cdot \frac{(bt)^{a-1} e^{-bt}}{\Gamma(a)}$$

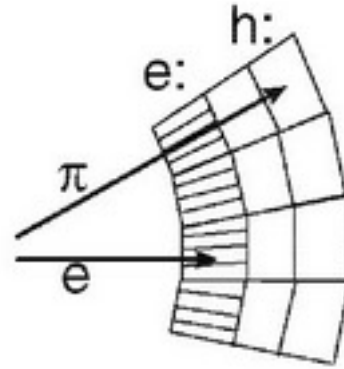
where

$$\Gamma(g) = \int_0^{\infty} e^{-x} x^{g-1} dx$$



(In dense media, the development of the shower is modified by the Landau-Pomeranchuk-Migdal (LPM) effect, a quantum mechanical effect which suppresses production of low energy photons. This must be considered at modern experiments such as those at the LHC.)

The **cascade is narrow** (Opening angle $\langle\theta^2\rangle \sim \gamma^2$ due to brem and pairs, and **increases** with depth due to multiple scattering of electrons, $\langle\theta\rangle \sim 1/E_e$.) Because showers broaden as they develop, calorimeters use projective geometry:



About **95% of a shower is contained within a cylinder about the axis, of radius $2R_M$** , where

$$R_M = \frac{21 \text{ MeV}}{E_c} X_0 [\text{g/cm}^2] \quad \text{is the Moliere radius.}$$

The **resolution of a calorimeter is approximately equal to the non-containment fraction**. Thus 5% non-containment translates to about 5% resolution.

The shower profiles have long tails: increasing the collection from 90% to 99% requires an order of magnitude more mass.

The energy deposited in the medium is due to the ionization losses of the charged particles \propto # of electrons and positrons.

To detect this energy, 2 processes are needed:

- 1) The energy is transferred from the particle to the medium – *“the particle is absorbed”*
- 2) *The energy is read out* - detected

Two options for EM calorimeter configuration:

- *homogeneous*: the absorber and the detector are combined
- *sampling*: the absorber and the detector are distinct

Homogeneous calorimeters – the full volume of the detector can absorb the energy and transmit it to readout

Measurement principle is any of these:

- detection of *scintillation* light (medium is scintillating crystals or liquid noble gas)
- collection of *ionization* (medium is liquid noble gas)
- generation of *Cherenkov* light (medium is heavy transparent crystal or lead glass)

The most important features of the calorimeter are the position and energy resolutions for photons and electrons.

Energy resolution:

$$\frac{\sigma_E}{E} = \frac{a}{\sqrt{E}} \oplus \frac{b}{E} \oplus c$$

crystal non-uniformity ($c < 1\%$)
electronics noise ($b \sim 100$'s of MeV)
photoelectron statistics ($a \sim 3\%-5\%$)

Notice: the resolution improves with increasing energy.

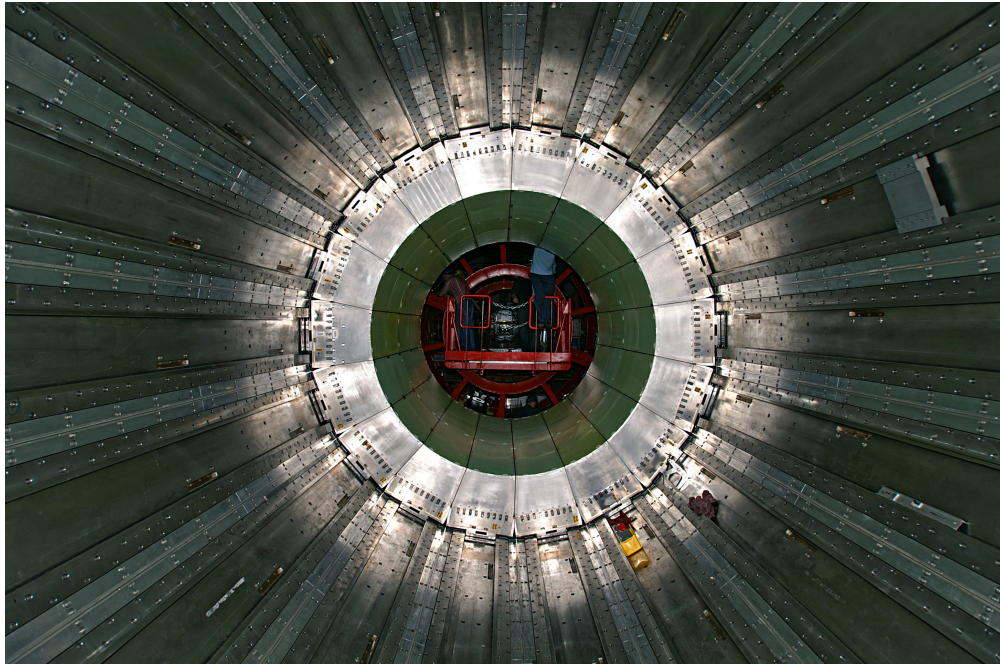


Example homogeneous calorimeter types:

1) **Crystal** calorimeters -best resolution at this time: $\sigma_E/E \sim 1\%$

(Lead glass calorimeters – less expensive than crystals, but lower Cherenkov light production increases resolution to $\sim 5\%/\sqrt{E}$)

2) **Ionization** calorimeters – often using noble liquids: liquid argon (LAr) is abundant, inexpensive, obtainable with high purity, radiation hard



CMS Ecal: 80k PbWO_4 (lead tungstate) *crystals*, mounted inside 4T solenoid: **Strengths:** short radiation length, small Moliere radius, fast scintillation emission, high radiation hardness. **Challenge:** low light output.

ATLAS LAr EM Calorimeter
(ionization principle)

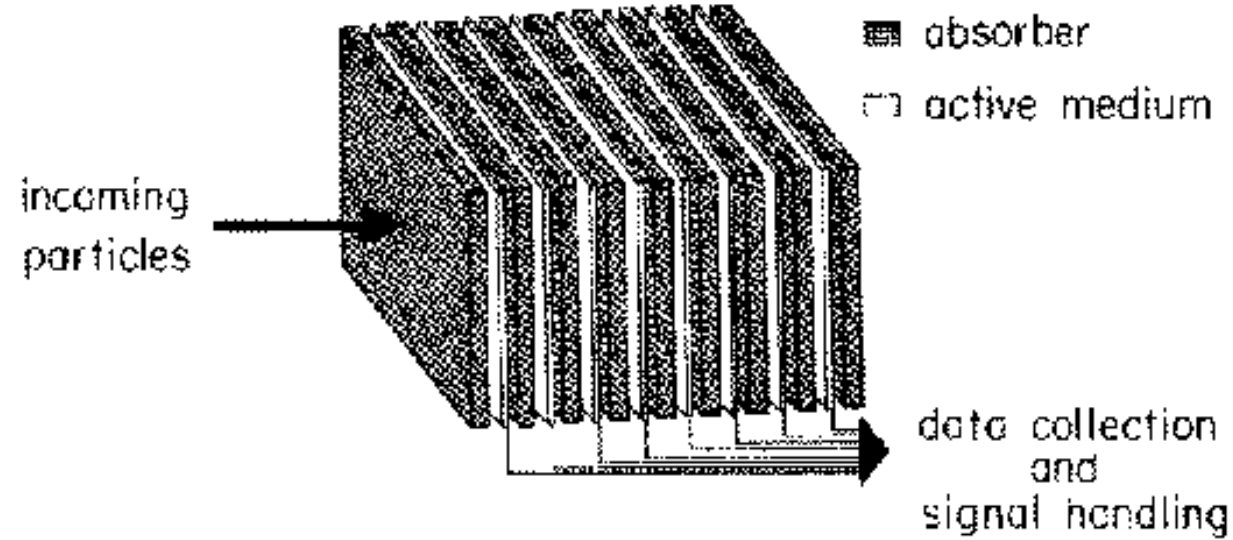


Calorimeter position resolution is taken from the corrected center of gravity of the energy deposition.
Approximately,

$$\sigma_{\text{longitudinal-position}} \sim \frac{R_M}{\sqrt{E/E_c}} \sim \text{few mm for } E_\gamma = 1 \text{ GeV with crystals}$$
$$\sigma(\theta) \sim \frac{\text{few mrad}}{\sqrt{E}}$$

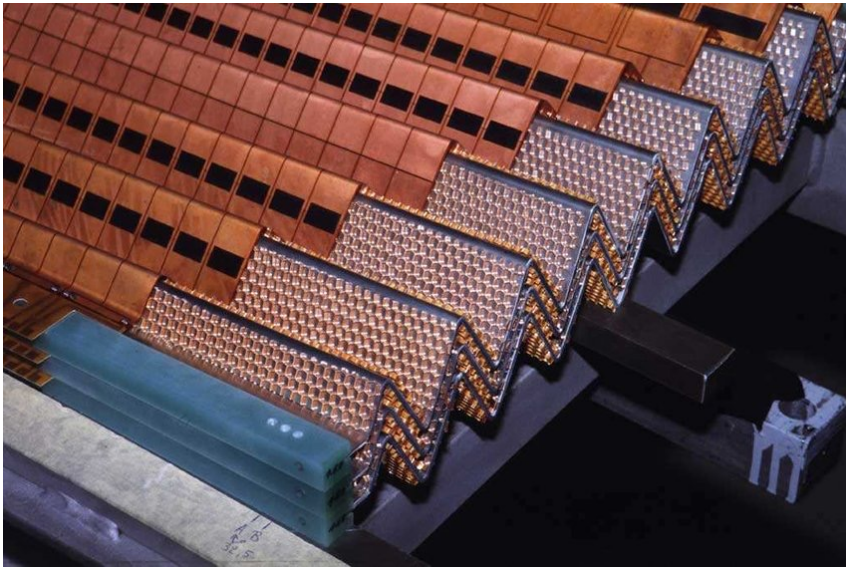
Sampling calorimeters – longitudinal stack of absorbers separated by thin counters

- **Typical sensors:** gas-filled ionization chambers, cryogenic noble gases (LAr, LXe) as ionization chambers, warm liquids, scintillators
- **Typical absorbers:** U, Fe, W, Cu, should be > 2 cm thick
- **Advantage:** each material can be separately optimized
- **Disadvantage:** contribution to resolution from sampling fluctuations (minimized in dense materials: typically $\sim 8\%$ in LAr @ 1 GeV).



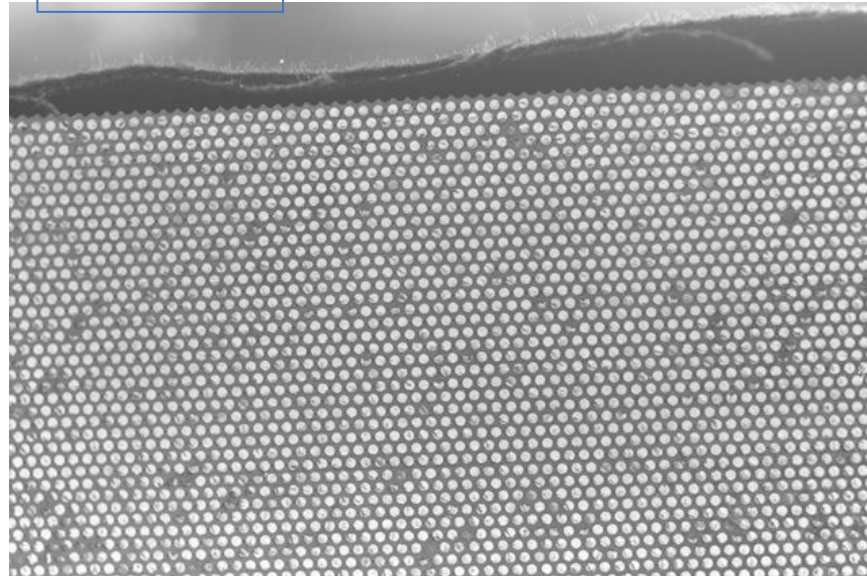
Sampling calorimeters, continued

Layers can be planes, or more complicated. To avoid “cracks” (gaps between adjacent towers): see the *accordion* chamber...



...and the *spaghetti* calorimeter, in which the counters are fibers embedded in the absorber...

KLOE Exp.



...and more geometries: shashlik-calorimeter, tile-calorimeter...

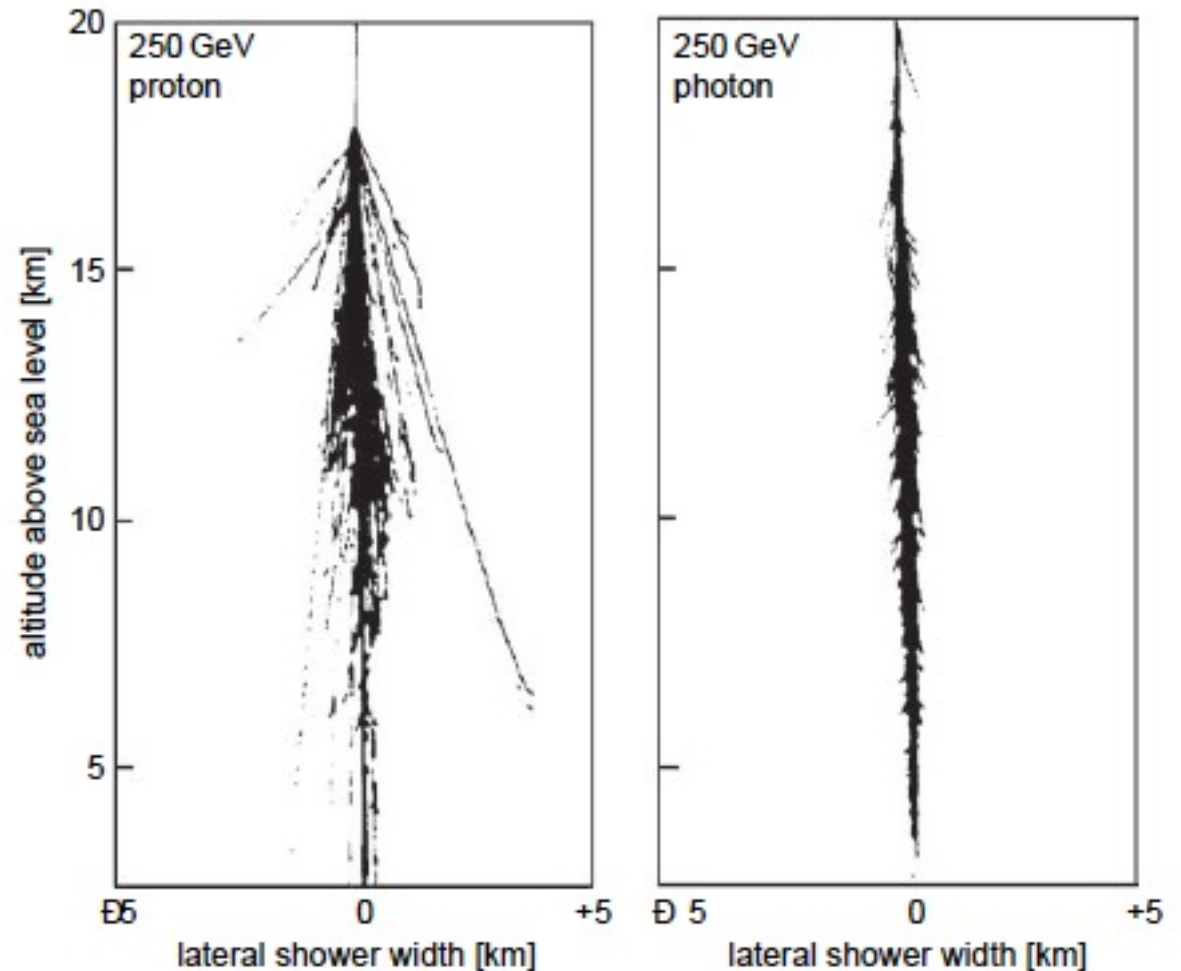
Hadronic calorimetry – to measure the energy of non-showering particles

- Similar geometries, but the *longitudinal shower development is determined by nuclear interactions*
- Showers include pions, kaons, nucleons
- Characterized by the *nuclear interaction length*:

$$\lambda_I \sim 35 \left[\frac{\text{g}}{\text{cm}^2} \right] A^{1/3}$$

This is longer than X_0 for most materials.

- Hadronic showers are broader than EM showers due to large transverse momentum transfers in nuclear interactions. Compare simulated air showers of equal-energy proton and photon.



How is the hadron energy dissipated in the absorber?

- 1/3 of the hadrons produced are π^0 . These decay quickly to photons, producing EM showers.
- Another 30%-40% of the hadron energy is dissipated invisibly as **broken nuclear bonds or production of stable neutrals** (neutrons, K_L^0).
- ***ONLY the EM energy dissipated by charged particles is recorded by any calorimeter***, so the hadron signal is smaller than the EM calorimeter signal, for the same particle energy. *Up to 40% of the non-EM energy may be “invisible”* – binding energy of nucleons released in nuclear reactions – with large event-to-event fluctuations.
- Large fluctuations in hadron shower development (i.e. fluctuations in number of π^0 's) leads to *worse resolution than in EM calorimeter*
- *Hadron calorimeters are intrinsically nonlinear with energy* – the average EM fraction (called “e”) increases with energy.
- The response of the calorimeter to the non-EM fraction (called “h”) is constant with energy. Thus:

$$\frac{e}{h} > 1$$

“**Compensation**” is a technique to recover information on the invisible energy, i.e. to achieve $\frac{e}{h} \rightarrow 1$

Only sampling calorimeters can be compensated.

Compensation methods:

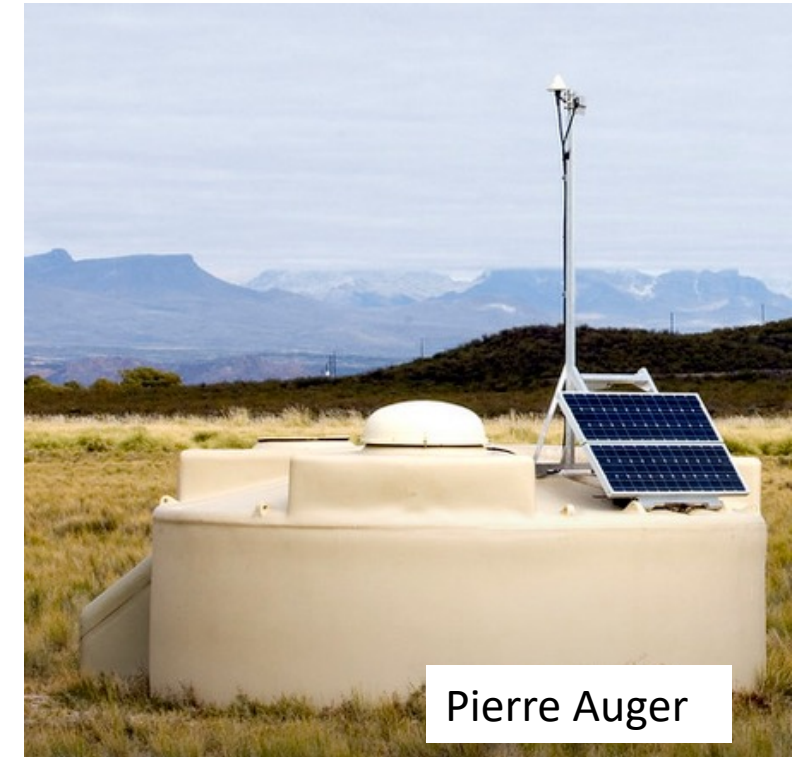
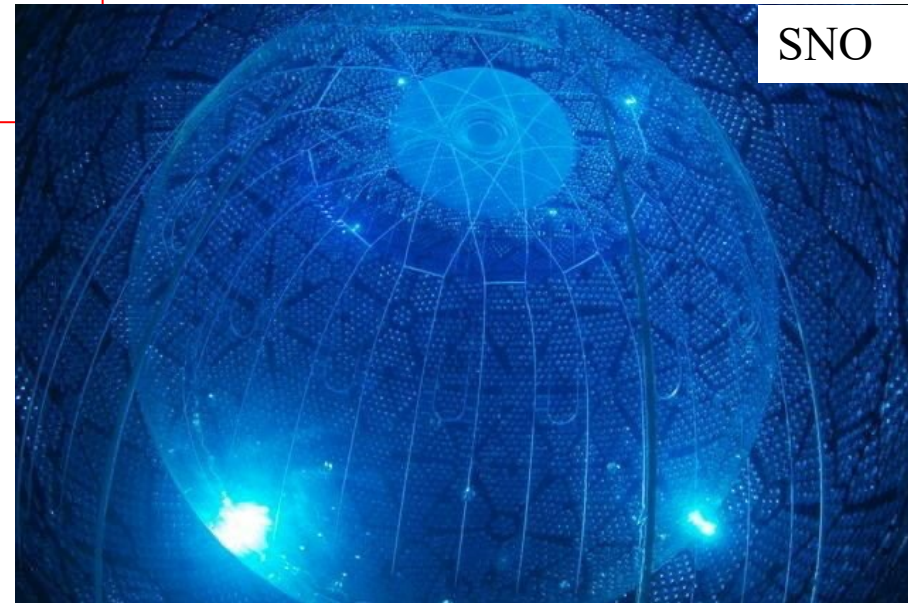
- *suppress the EM response* (e.g. choose high-Z absorber material)
- *boost the non-EM response* (choose an absorber containing hydrogen; incoming neutrons recoil on the protons, which then contribute to the signal)
- “*offline compensation*” – determine the energy sharing between EM and hadronic components on an event-by-event basis through analysis of event characteristics (shower shape, composition) – this is “Dual REadout Method” (DREAM) calorimetry.
- uranium absorber – *fission materials liberate additional energy*

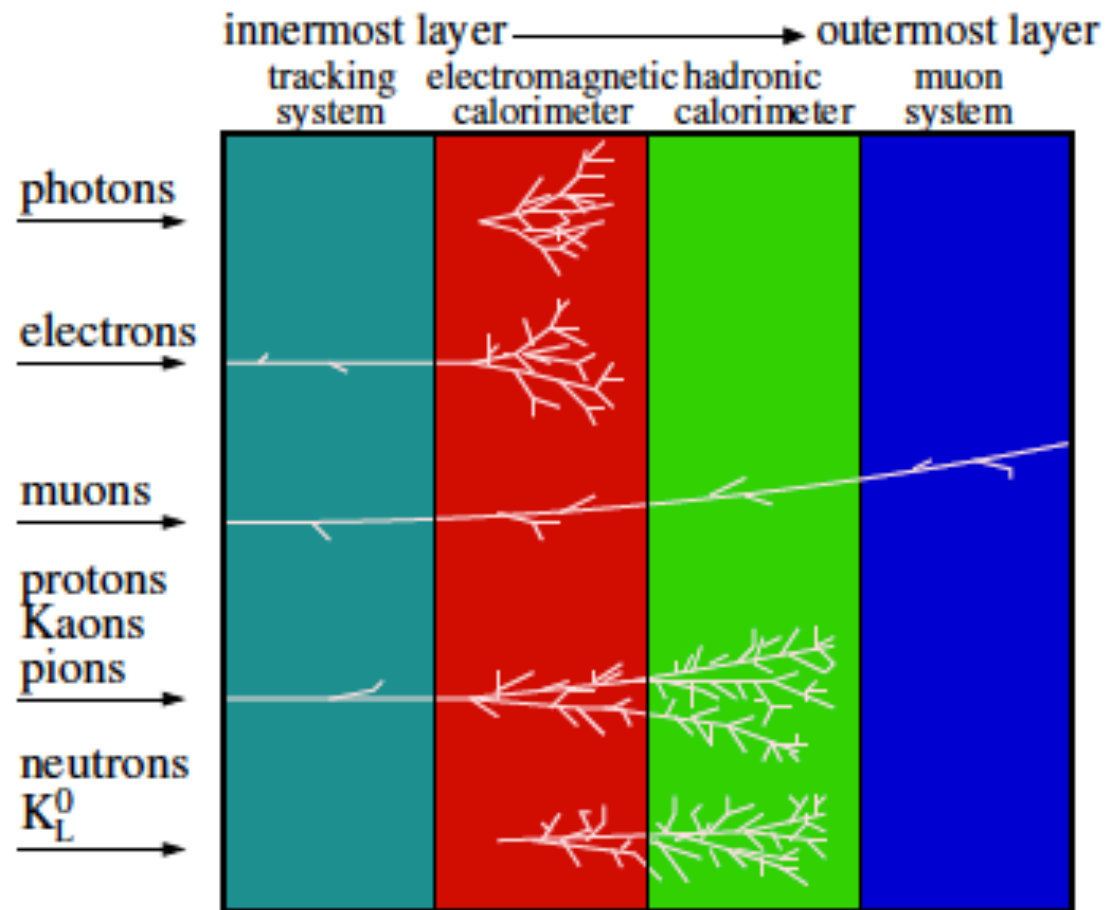
ZEUS (uranium/scintillator) achieved $\frac{\sigma}{E} \sim \frac{35\%}{\sqrt{E}}$. ATLAS (non-compensating) “Tile” calorimeter achieves $\frac{\sigma}{E} \sim \frac{42\%}{\sqrt{E}}$

Calorimetry applications outside the realm of particle accelerators:

- energy measurements of *extensive cosmic ray showers induced in the atmosphere*: detect scintillation or Cherenkov light (Pierre Auger, HiRes Fly's Eye).
- energy measurements of cosmic neutrinos or muons: "*neutrino telescopes*" employing photo detectors in a matrix of absorber deep underground or in the sea (Kamiokande, IceCube, SNO).
- detection of *extremely low energy particles* (e.g. hypothesized WIMPs). This requires cryogenic operation to suppress thermal noise.

Phonons provide a signal in the μeV to meV range, detectable with classical calorimetry via energy deposition in an absorber (CRESST detectors, CYGNUS, DRIFT)





Particle Identification

First, particles are roughly identified by comparing their signals in the different subsystems (previous slide)

Tracking system:

- Determines the sign of the charge by the direction of curvature in magnetic field
- Images decays of some charged particles via kinks ($K^+ \rightarrow \mu^+ \nu$)
- Identifies heavy quarks by secondary vertices
- Distinguishes “V” particles: neutrals (K^0_s , Λ , anti- Λ) that decay to 2 charged particles, whose track forms a V

Calorimeter:

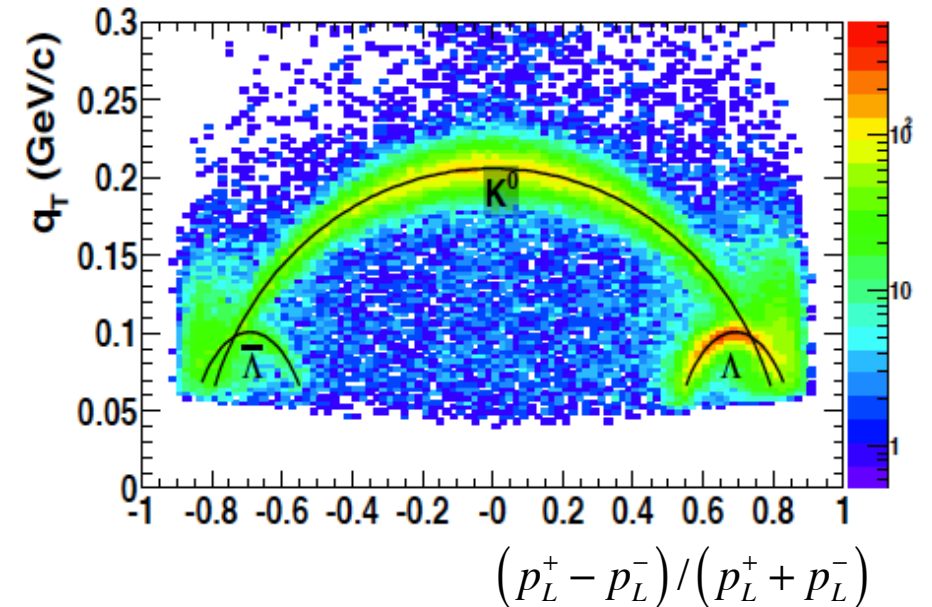
- Photons and electrons produce identical showers in EM calorimeter, but photons are invisible in the tracking
- Hadrons deposit most but not all of their energy in the hadron calorimeter

Muon Detector:

- Unique for one particle type, because muon mass (200 x electron mass) inhibits it from showering in the EM calorimeter. Muon is not a hadron, so it passes through both calorimeters largely unaffected, to reach muon system beyond them.

Neutrinos:

- Do not interact strongly or electromagnetically so must be inferred by apparent imbalance of observed energy, momentum



The challenge is to distinguish particles that have similar interactions in the same subsystem. For example: protons, charged pions, charged kaons.

This must be done through **particle ID by mass.**

$$\text{Because } p = \gamma m v,$$
$$m = \frac{p}{c\beta\gamma}$$

The approach: *measure p with a tracking chamber, then find velocity β using one of these methods:*

- Time-of-flight
- Specific ionization
- Cherenkov images
- Transition radiation

A different approach: *features of the showers they produce in calorimeters*

Time-of-flight (TOF)

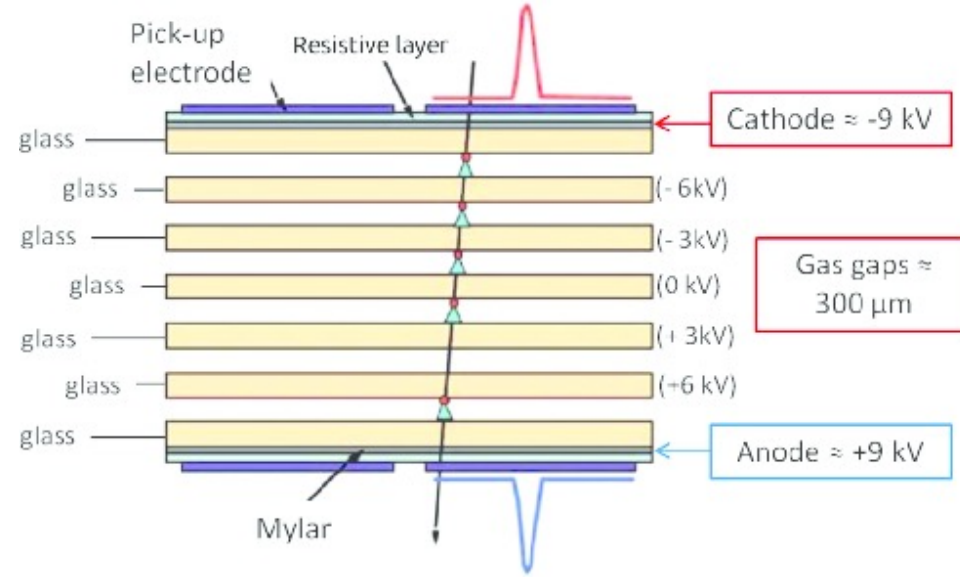
Notice:

$$\text{Velocity } \beta = \frac{1}{\sqrt{\left(\frac{m_0 c}{p}\right)^2 + 1}}$$

"Equation 1"

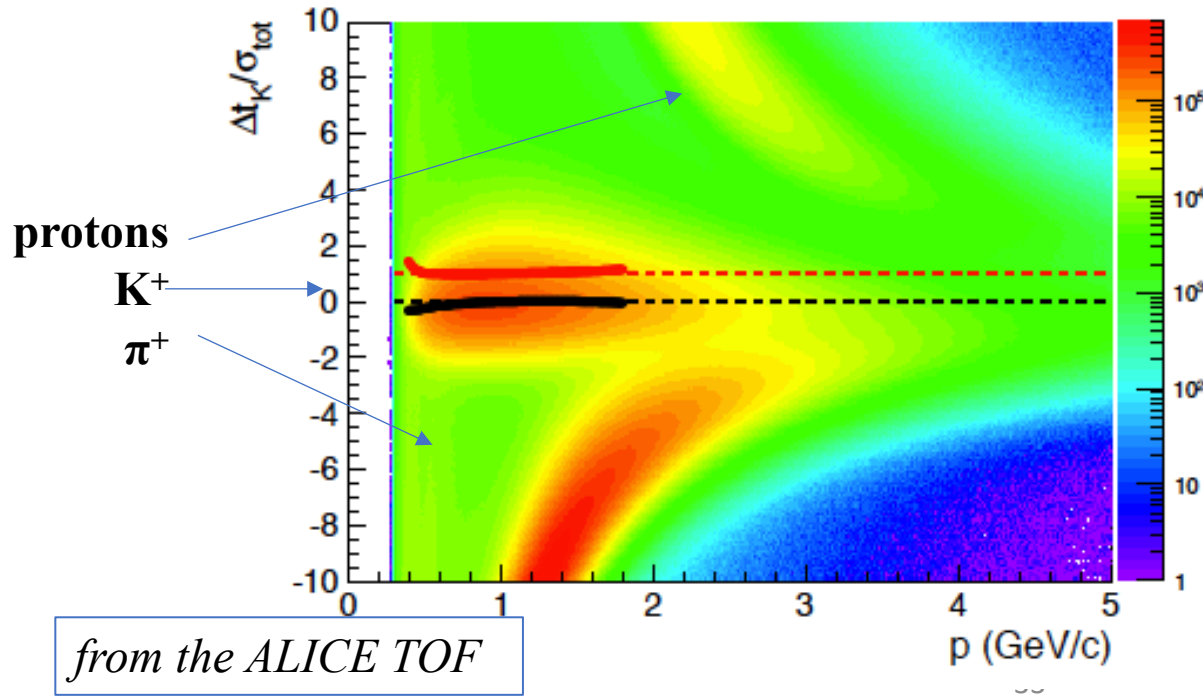
$$\text{so } m = \frac{p}{c} \sqrt{\frac{c^2 t^2}{L^2} - 1}$$

Combine time t measurement with momentum p and track length L from tracking detectors.

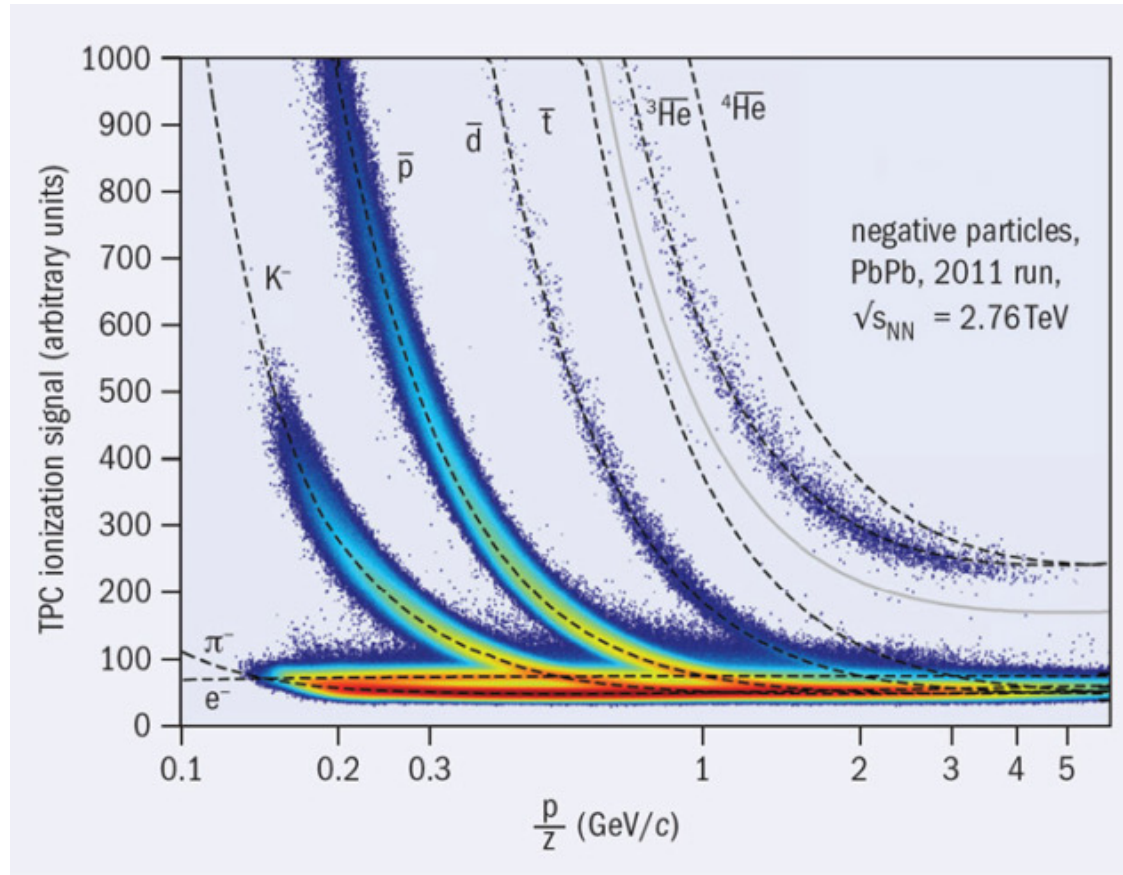


Multigap Resistive Plate Chambers (MRPCs) – a gaseous parallel-plate avalanche detector.

- Electrodes have high volume resistivity.
- Gas gap between the electrodes is subdivided by internal plates – physical barriers that stop the avalanche from growing too large. On the order of ~5 gas gaps each ~250 microns wide.
- This allows the applied E field to be very intense without risk of breakdown
- Compare time of TOF trigger to time of event.
- Fine time resolution and rate capability.



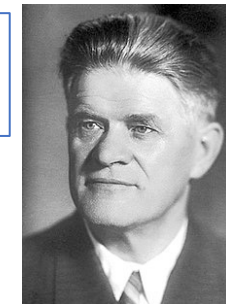
Rate of ionization energy loss – dE/dx :



- Can be read from pulse heights in gaseous or solid state *proportional* chambers
- Follows from the *Bethe-Bloch* formula
- Usefulness diminishes for $p \gtrsim 1 \text{ GeV}$

from the ALICE TPC

Nobel Prize in Physics 1958: Pavel Cherenkov, Ilya Frank, and Igor Tamm



Cherenkov radiation imaging

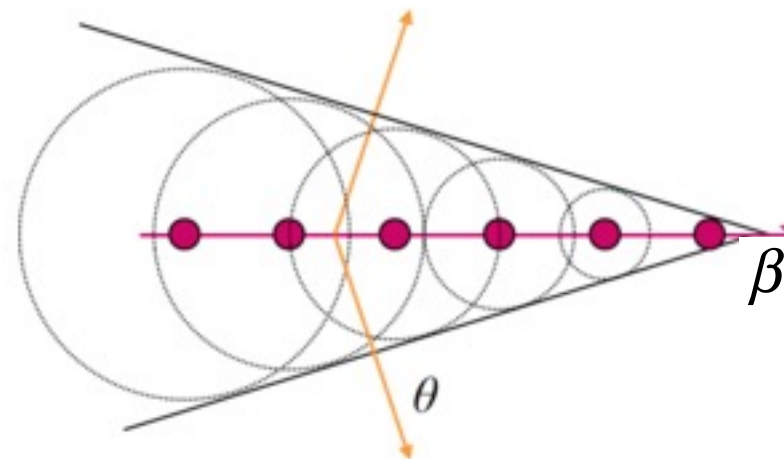
Recall from Lecture 2, when a charged particle travels through a medium with velocity that is greater than the velocity of light in that medium, coherent wavefronts of light are emitted.

The angle θ the wave fronts make with the path of the the particle depends on the particle velocity β and the index of refraction, which also depends on the photon energy – $n(E)$:

$$\cos \theta = \frac{1}{\beta n(E)}$$

Combine this with Equation 1 from Slide 5 to get:

$$m = \frac{p}{c} \sqrt{n^2 \cos^2 \theta - 1}$$



Particle physics experiments use the Cherenkov effect in *several types* of particle-identification detectors:

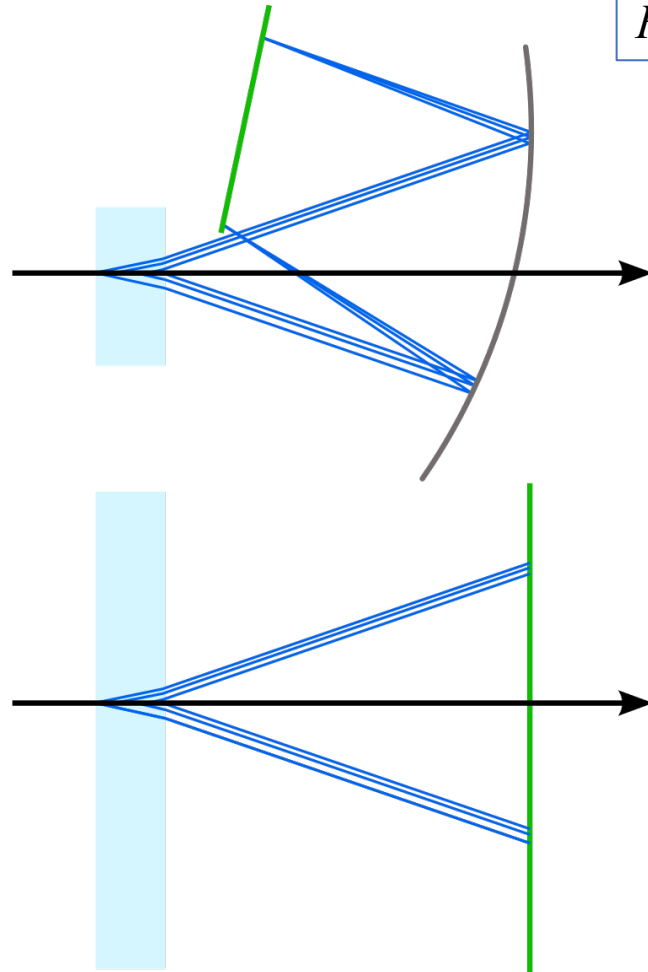
- Imaging Cherenkov counters
 - Ring-imaging Cherenkov (“**RICH**”) including Imaging Atmospheric Cherenkov Telescopes (**IACT**)
 - Detection of Internally Reflected Cherenkov (“**DIRC**”)
- **Threshold** Cherenkov counters
- **Differential** Cherenkov counters

Recall that all require *a radiator* and *a photon detector*.³⁵

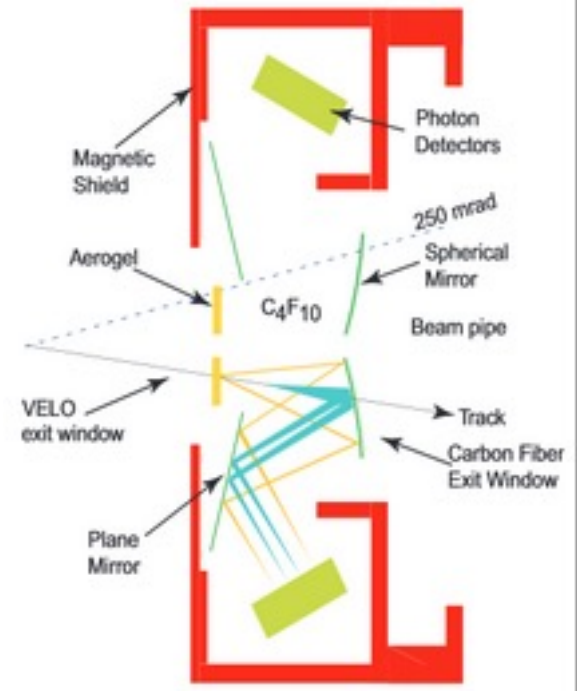
RICH detectors – for use in a collider environment where the tracks can be emitted *over the full solid angle*

The **radiator** can be:

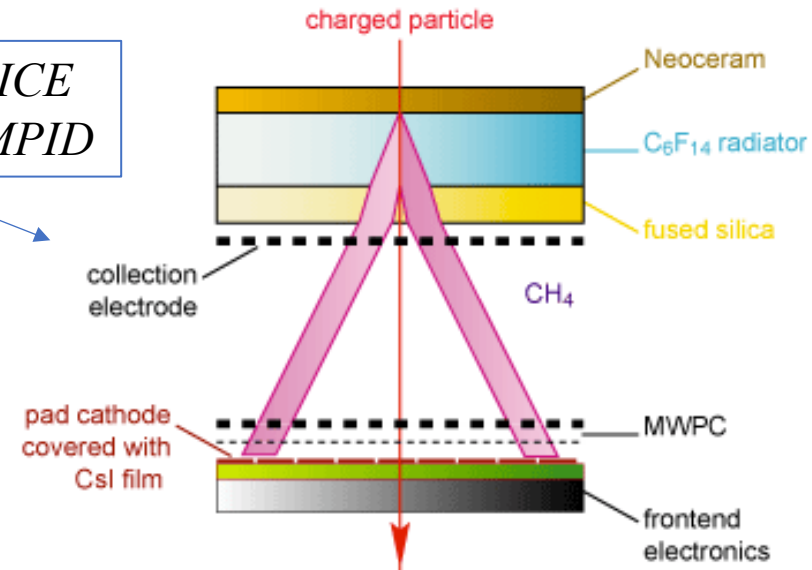
- **gaseous (low index n), then thick (~50 cm) to produce sufficient light.** The light is focused by spherical or parabolic mirrors onto photon detectors where ring-shaped images are formed.
- **dense (high index n), then thin (~1 cm) will be sufficient to produce enough photons.** The photosensor is located ~10 cm behind it (“the expansion gap”), to allow the light cone to develop directly on the photon detection plane



LHCb
RICH



ALICE
HMPID



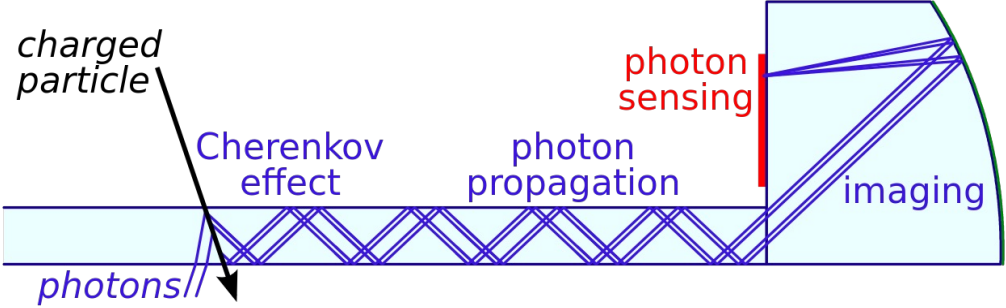
In the **DIRC**, light that is captured by *total internal reflection inside a solid radiator* reaches the light sensors at the detector perimeter. This is different from a classic RICH which uses the transmitted light. In the DIRC, the radiator is also the light guide. The precise rectangular cross section of the radiator *preserves the angular information* of the Cherenkov light cone.

Example **Threshold Cherenkov Detector**, where the mass-dependent threshold energy *discriminates between light particles (which radiate) and heavy particles (which do not)*.

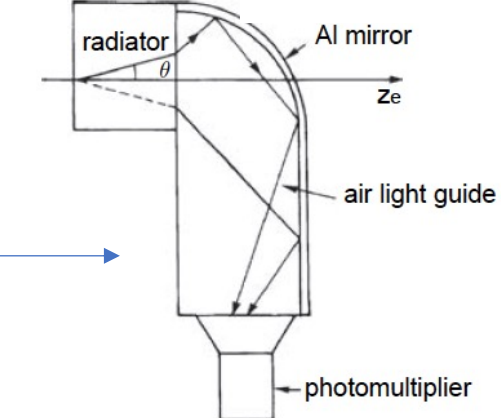
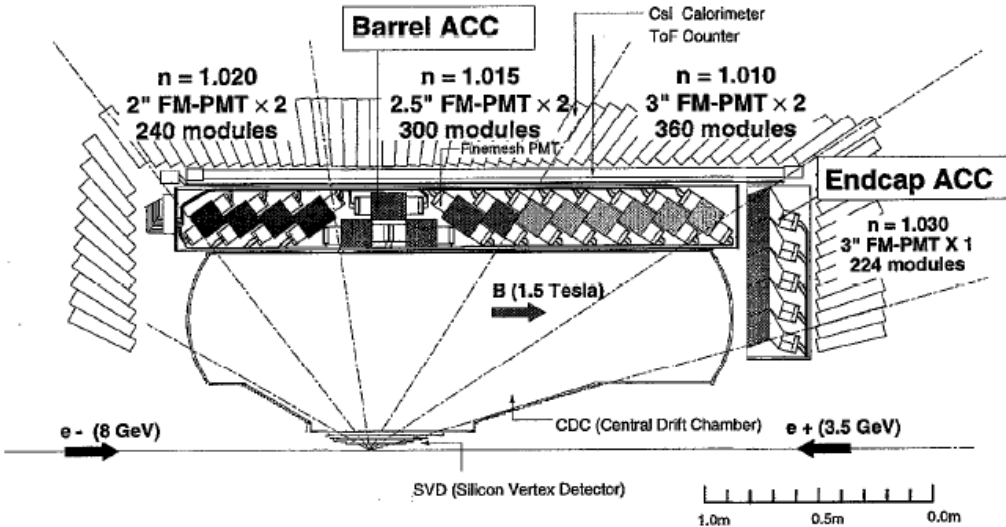
- Particle energy is measured (count # photoelectrons)
- For known energy, velocity β depends on particle mass
- Radiation is only emitted if $\beta > 1/n$, so light particles are distinguished from heavy

Differential Cherenkov Detector: in which *particle velocities are measured by their ring opening angle*. Schematic differential, or “Fitch-type” Cherenkov detector selects a specific velocity range.

BaBar Expt.

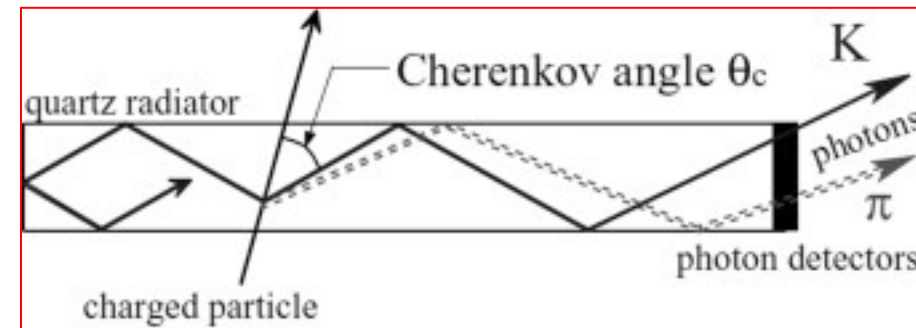
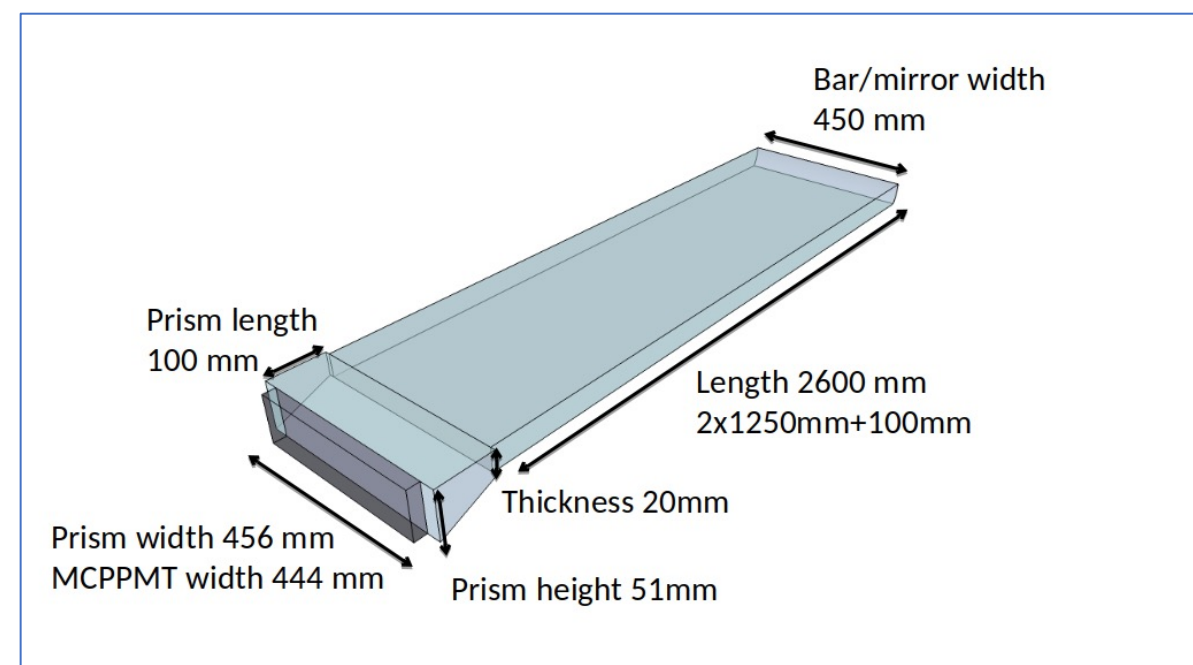


Belle aerogel



Add precision timing information to the DIRC:
The Belle TOP (Time of Propagation Cherenkov Detector)

- quartz radiator bars: one end of the bar has a spherical mirror to reflect light back to the other end that has a small expansion prism.
- The prism is instrumented with MCP-PMTs read out with custom fast sampling: the time of arrival of each photon is measured with sub-50 ps timing resolution.



Application of Cherenkov imaging to astrophysics:
Imaging Atmospheric Cherenkov Telescopes
detect very high energy (50 GeV – 50 TeV) gamma rays

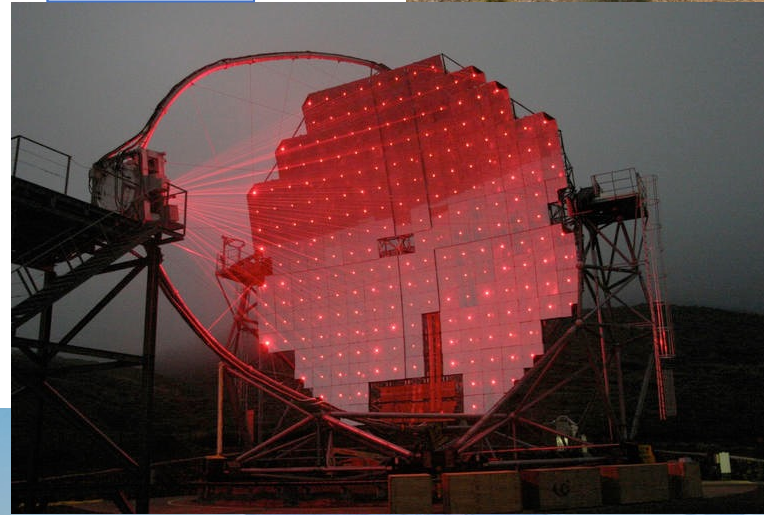
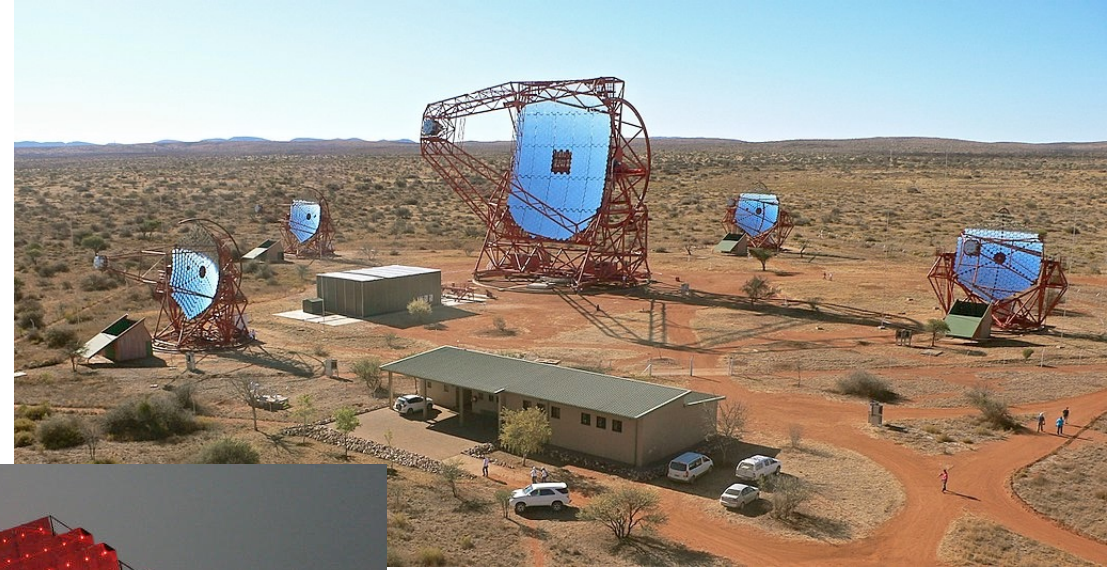
*When the gamma ray strikes the atmosphere, it converts to an EM shower. The entire atmosphere functions as the **radiator**. The detector is a segmented mirror that reflects the Cherenkov light onto a PMT array which is the **detector**.*

Background suppression: The shower triggers multiple detectors, distinguishing itself from local muons which are observed only in single detectors.

A history of these instruments:

- Whipple
- HEGRA
- MAGIC
- H.E.S.S.
- FACT
- Veritas
- MACE

MAGIC

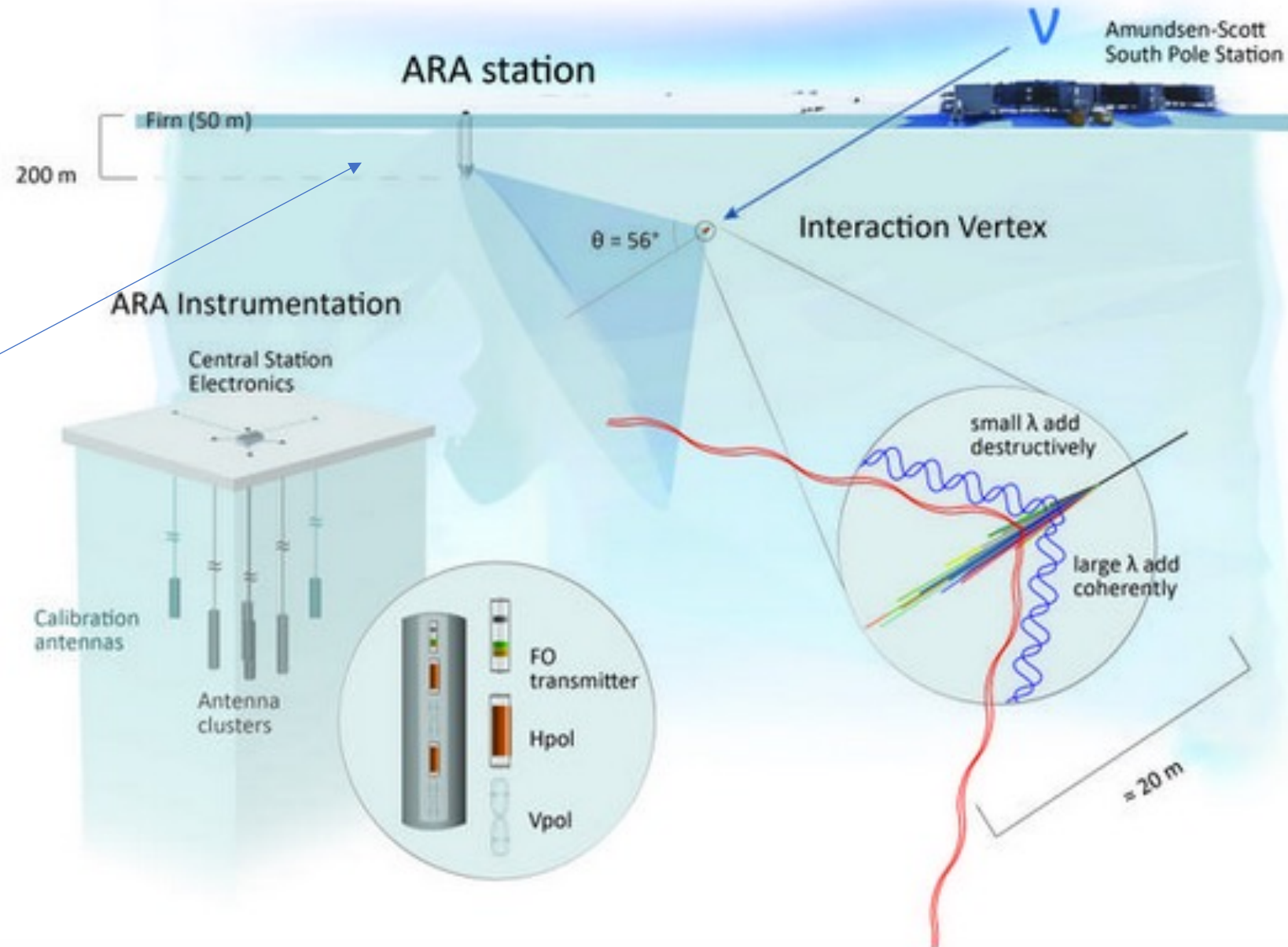


H.E.S.S.

Veritas



*Cherenkov emission also occurs at radio wavelengths when EM showers occur in dense media (ice, sand, lunar surface) – then it is called the **Askaryan effect** and is used to detect neutrinos (see next section of this lecture)*

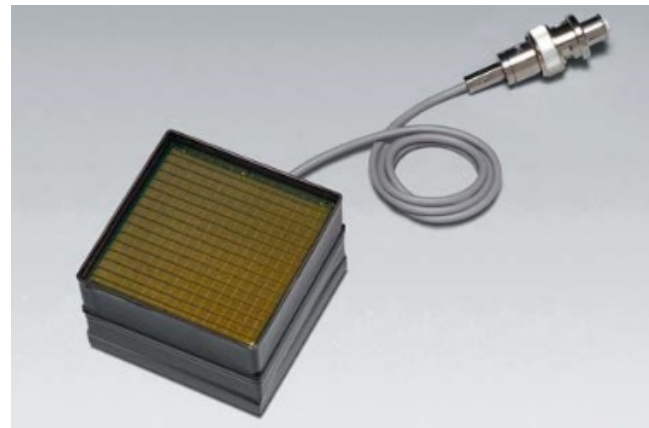
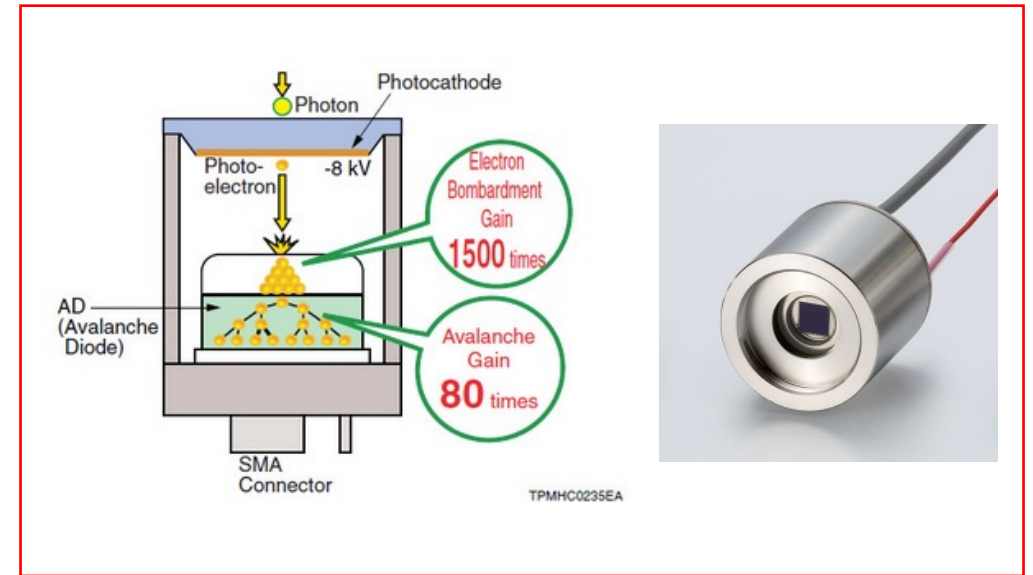


Requirements on the **photon detectors** (not the radiators) of the Cherenkov photons:

- *fast* enough to keep up with e.g. LHC bunch crossings
- *sensitive* to single photons
- *large* area coverage

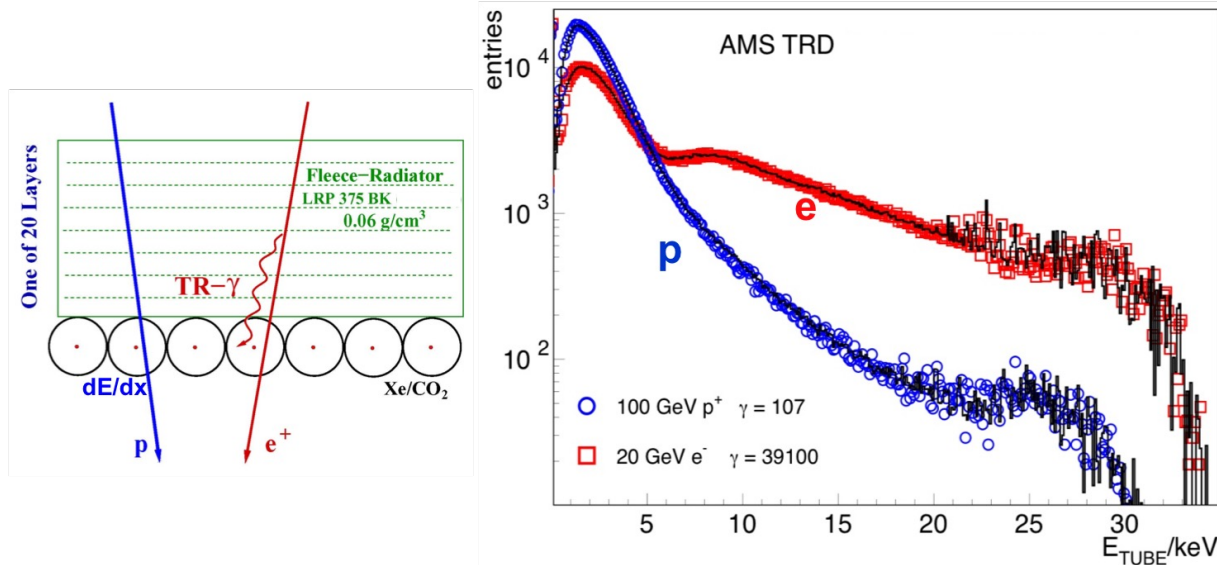
Some technologies that have worked:

- **Hybrid Photon Detectors** (HPD): photon converts in a quartz window with photocathode, then photoelectrons are accelerated through a gap to a silicon pixel chip. [LHCb]
- Special **photomultiplier tubes** (PMT's) for large neutrino experiments [SuperKamiokande]
- **Multi-anode PMT's** [COMPASS Experiment]

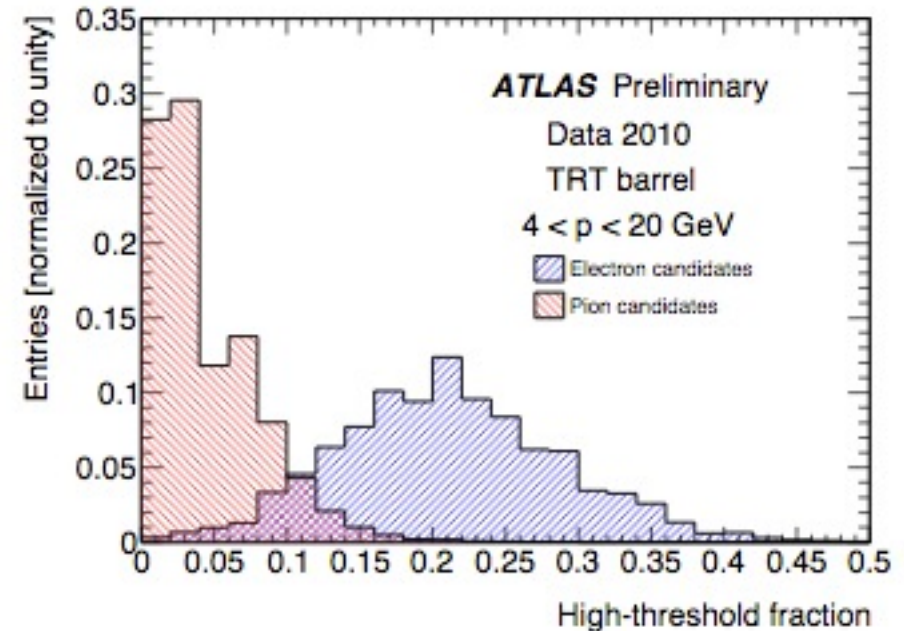
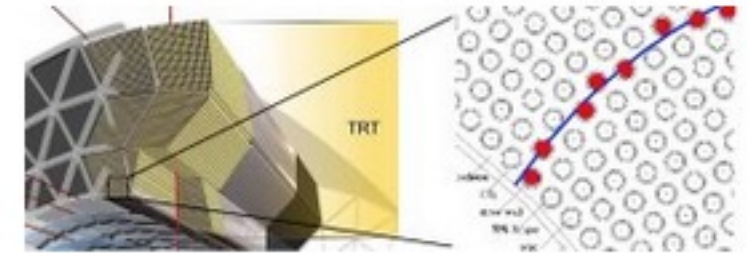


Transition Radiation Detection (recall Lecture 2, slide 24)

Example from the AMS Experiment: Gas proportional tubes are placed directly after the TRD. Protons deposit energy in the tubes, while electrons produce transition radiation that is detected there.



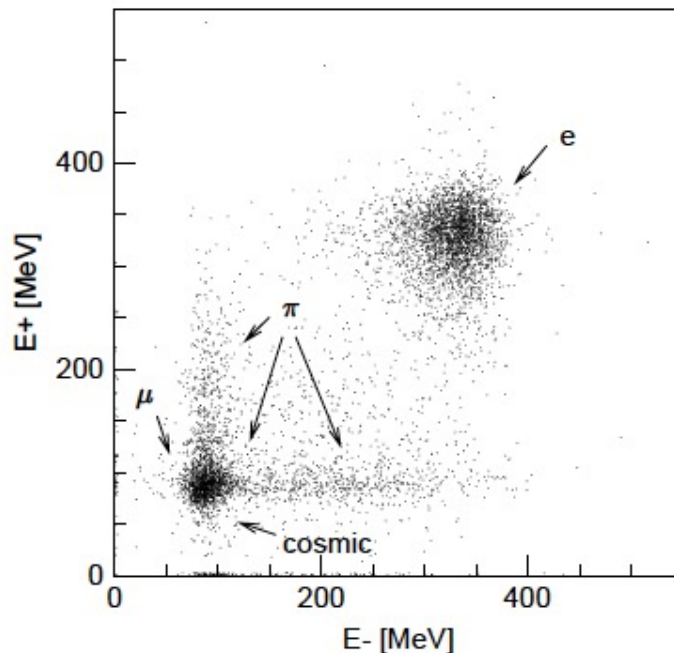
Example from ATLAS Transition Radiation Tracker (TRT) – a straw tube matrix, providing 30 space points with resolution ~ 130 microns on every charged track. Operating in drift chamber mode, the signals from tracks are compared to threshold values that distinguish electrons from charged pions.



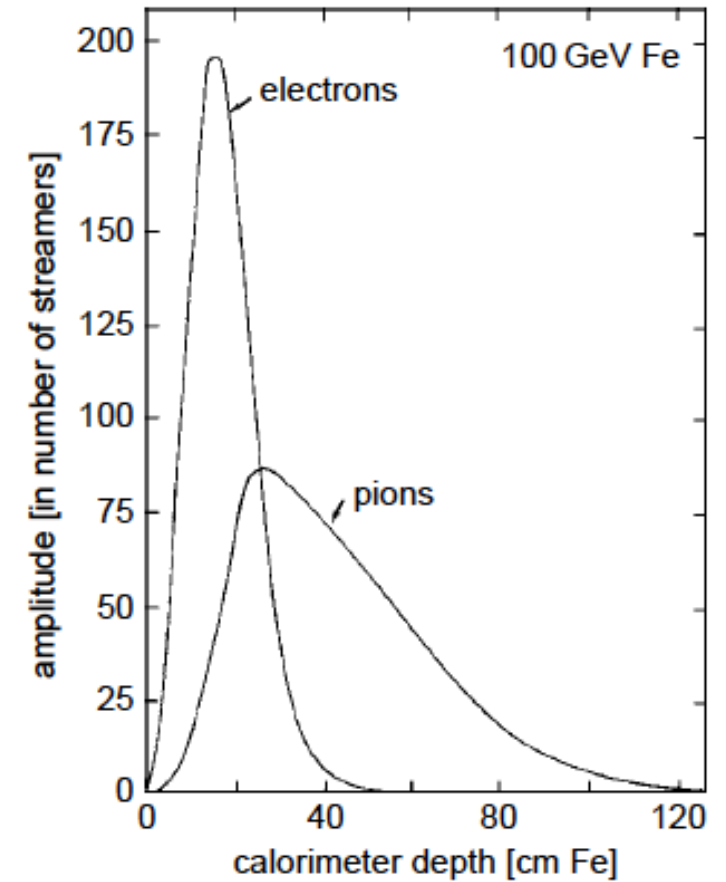
Calorimeter-based particle identification: Distinguishing electrons from hadrons on the basis of their *longitudinal and lateral shower profiles*

- Ratio of deposited E vs. p in the EM calorimeter distinguishes electrons from hadrons
- Starting point, and longitudinal center of gravity, of shower development separates electrons from pions
- Hadronic cascades are $\sim 5x$ wider than electromagnetic ones

Typically these profiles are combined into a *likelihood function* that is applied to any signal of interest.



Separation quality in events with two identical mass, opposite-charge particles in the final state, for a CsI crystal calorimeter.



Longitudinal development of 100 GeV particles in a streamer-tube iron calorimeter.

But: at the highest energies, muons brem (emission of EM radiation) leading to some misidentification.

Neutron identification – *relevant for dosimetry but not applied to high energy physics experiments*

It's always *indirect* – ***charged particles have to be produced*** in the neutron interactions, and then observed using the techniques already described: *ionization, scintillation*.

A neutron counter always includes ***an anti-coincidence counter*** (that vetoes incoming charged particles) ***followed by a neutron detector***.

The lower the neutron's energy is, the higher the cross section for detection, so often there is a ***moderator*** (a medium that reduces the speed) included.

Detection techniques:

- *Absorption*: neutron is incident on Li, B, He, H, or U, resulting in emission of proton or alpha
- *Activation*: neutron reacts with absorber (In, Au, Rh, Fe, Al, Nb, Si) to produce reaction products that subsequently decay to beta or gamma
- *Elastic scattering*: hydrogenous target is ionized, ions are detected.

Then eventually, detection of the products with proportional counters, scintillation counters, and solid state detectors.

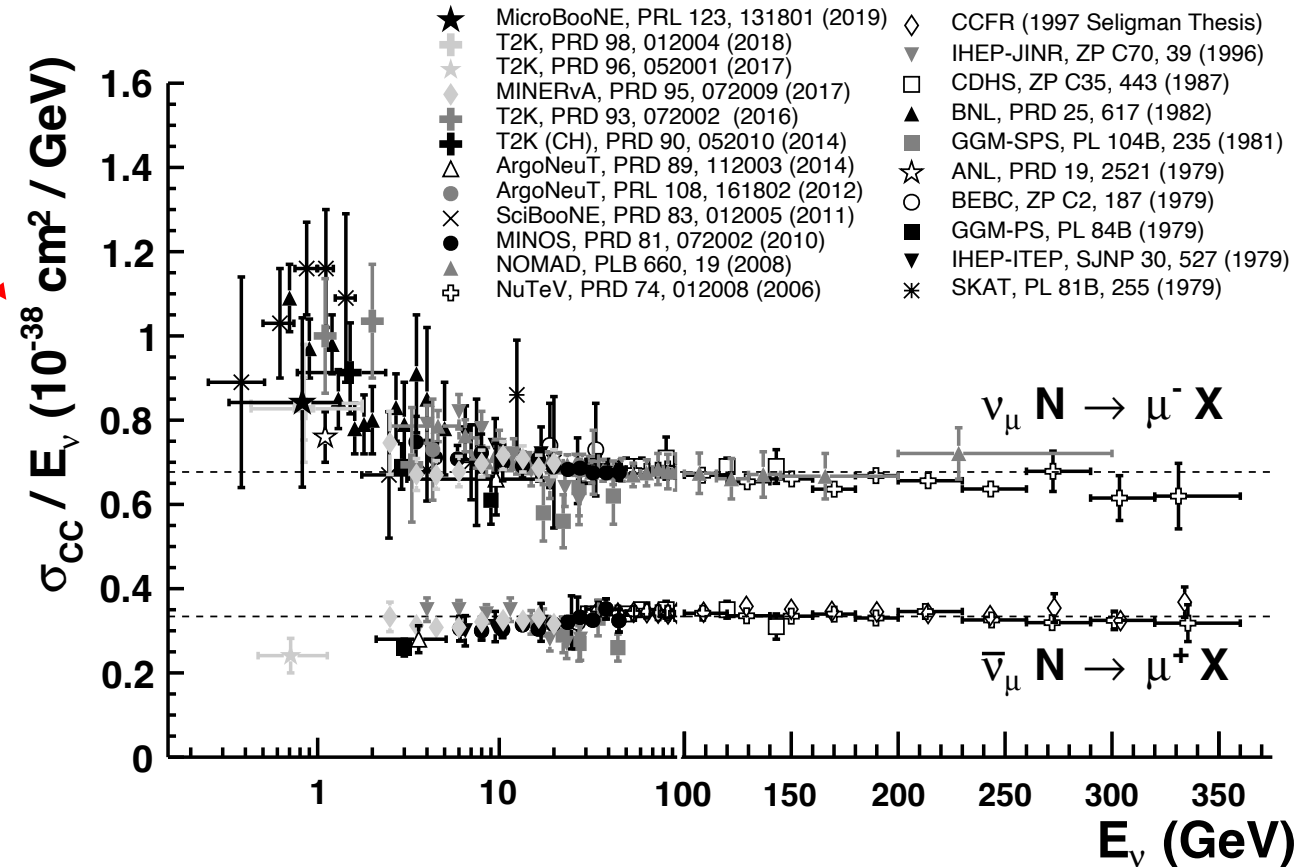
Neutrino Detectors

Neutrino cross sections are very, very small, so the *options for detecting neutrinos are*

- provide *high neutrino flux* and/or
- use an *extremely massive target*, to obtain charged particles, excited nuclei, or excited atoms produced by neutrino interaction. These can then be detected by standard means

-or-

- infer the presence of a neutrino by the absence of *quantities that it carries away* - energy, momentum – but which are expected to be conserved.

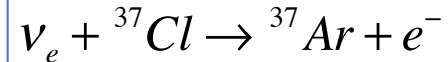


Note: *neutrino detectors rely on indirect measurement* – they measure the characteristics not of the neutrinos, but of the products of their interactions. They use all the same technologies as have been presented up to this point.

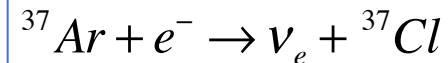
Examples for the “high flux, massive target” strategy:

- “*Radiochemical experiments*” – Counting neutrinos by *counting the products of their reactions*:

In the Homestake (solar neutrino) experiment, chlorine in the detector permitted the reaction



The argon was removed from the detector where it underwent



which is excited chlorine, which then decayed to x-rays or Auger electrons that were counted (with proportional tubes, etc.) as the signal.

Analogously for the GALLEX and SAGE experiments.

These experiments have primarily studied solar neutrinos.

- ***Calorimetric neutrino detectors*** measure the energy of the final state hadrons produced in the neutrino-nucleon interaction.

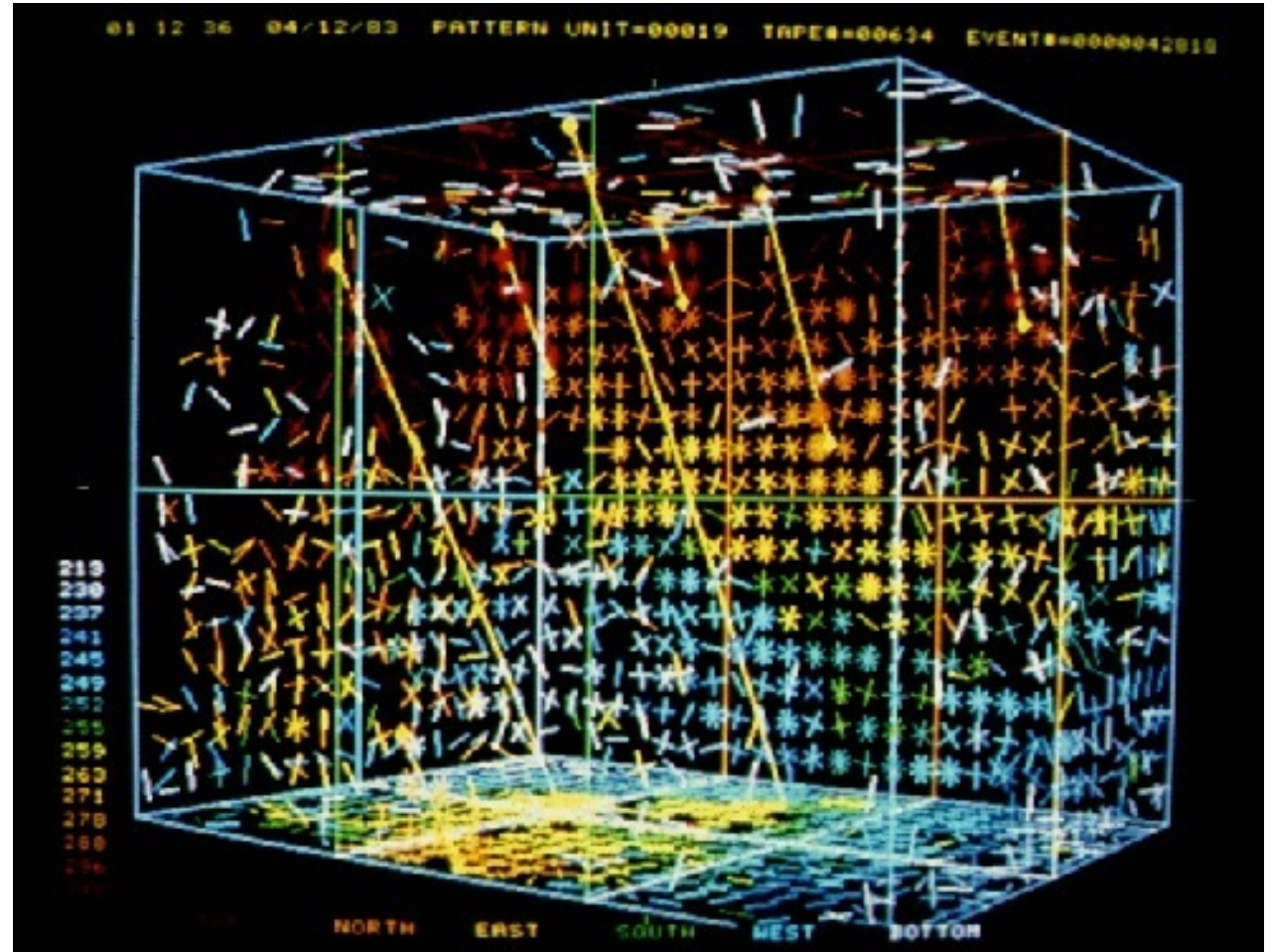
The detectors are *hadron calorimeters*:

- *sampling* sandwiches of alternating passive (dense) and active (scintillator) materials [CDHS, CHARM experiments] that measure energy and momentum, or
- large *homogeneous* total-absorption devices that detect the **Cherenkov light** [SuperKamiokande, SNO], **scintillation light** [KamLAND, KATRIN liquid scintillator], or **ionization electrons** [DUNE Far Detector liquid argon]. These are complete experimental detectors that:
 - reconstruct track patterns
 - measure energy
 - vertex events
 - identify charged particles (non-showering particles make sharp rings, showering particles, diffuse ones)
 - reject backgrounds
 - self-trigger

Cherenkov-light imaging detectors use the Cherenkov cone information to *reconstruct the tracks* of the products from neutrino interactions to provide *complete event reconstruction* for neutrino astronomy.

These require enormous volumes of transparent materials:

- water (SuperKamiokande, IMB)
- ice (IceCube, AMANDA)
- sea water (ANTARES)



Particle tracks reconstructed from Cherenkov rings detected by photomultiplier tubes on the walls of the water-filled IMB detector.

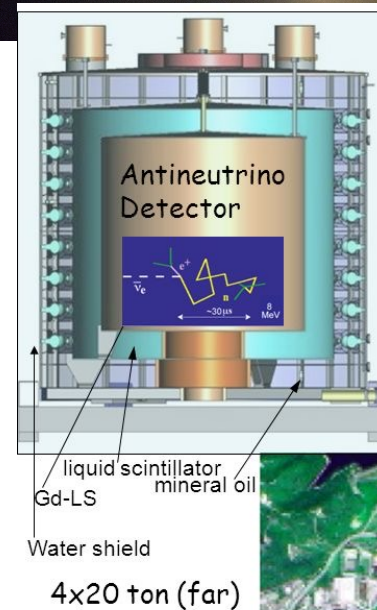
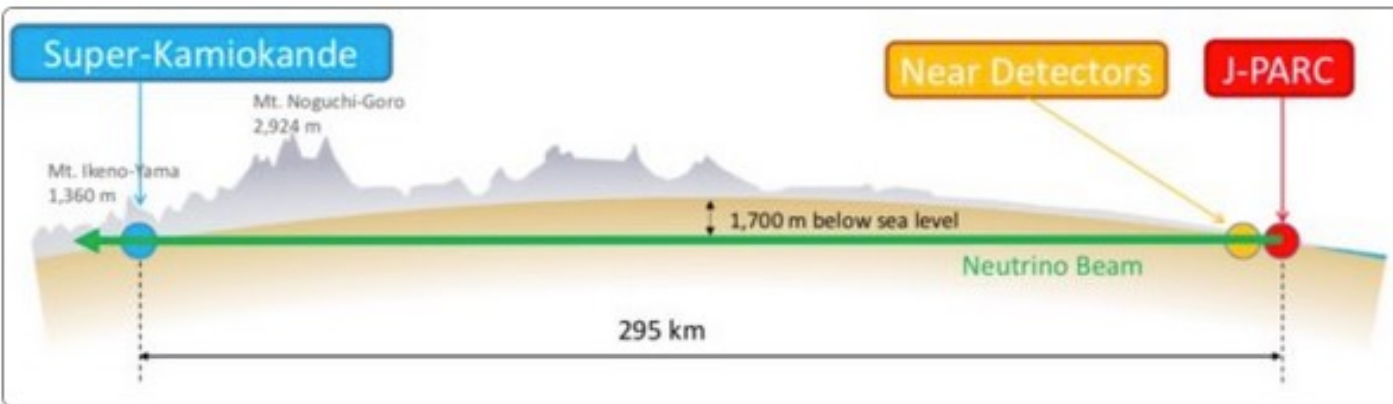
The neutrino flux may come from *extra-terrestrial sources* [IceCube], *accelerators* [NOvA and DUNE in the Fermilab neutrino beam; T2K is Kamiokande in the Tokai muon neutrino beam], or *reactors* [Daya Bay].



T2K



Daya Bay



Water shield
4x20 ton (far)



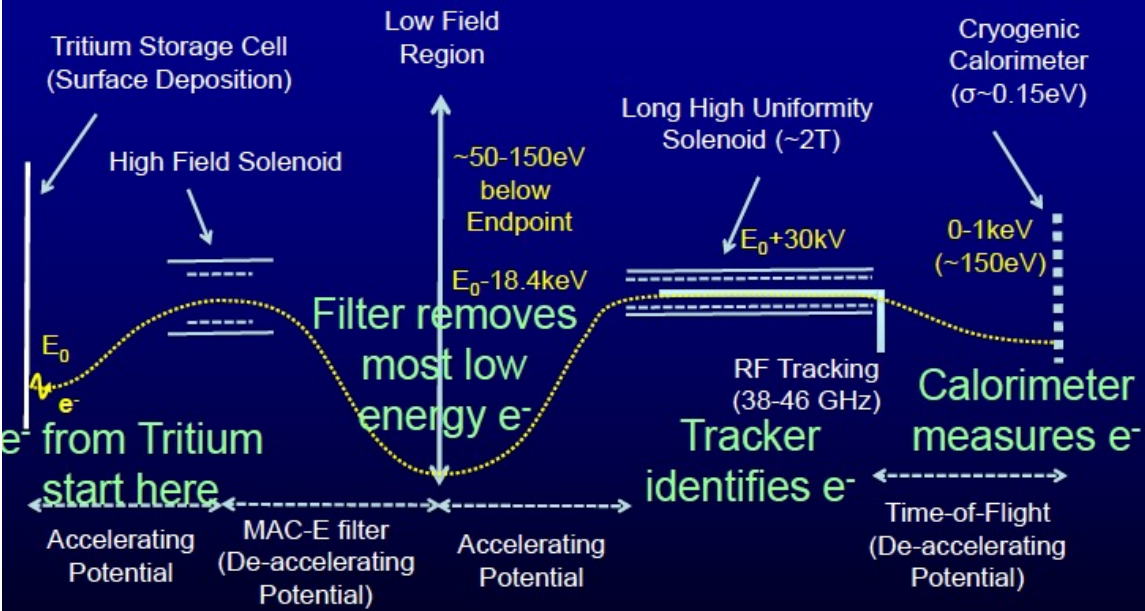
Detectors intended for cosmic neutrinos are uniquely enormous, to overcome the problem of low flux.

Examples:

- *AMANDA/IceCube* are arrays of PMTs embedded in South Pole ice, depth 1500 - 1900 meters, array diameter 200 meters, to detector Cherenkov light
- *ANTARES (and future Km3NeT)* are arrays of PMTs in the Mediterranean sea
- *Askaryan Radio Array (ARA)* uses radio receivers embedded in South Pole ice to detect radio-frequency Cherenkov emissions from neutrino interactions in the ice.
- *AMANDA2 at the South Pole* records signals from “upward-going” muons produced by neutrinos interacting while traversing the earth’s volume.

And there is a technology proposed for detecting *neutrinos from the Big Bang* (CNB – “cosmic neutrino background”): **the PTOLEMY project**.

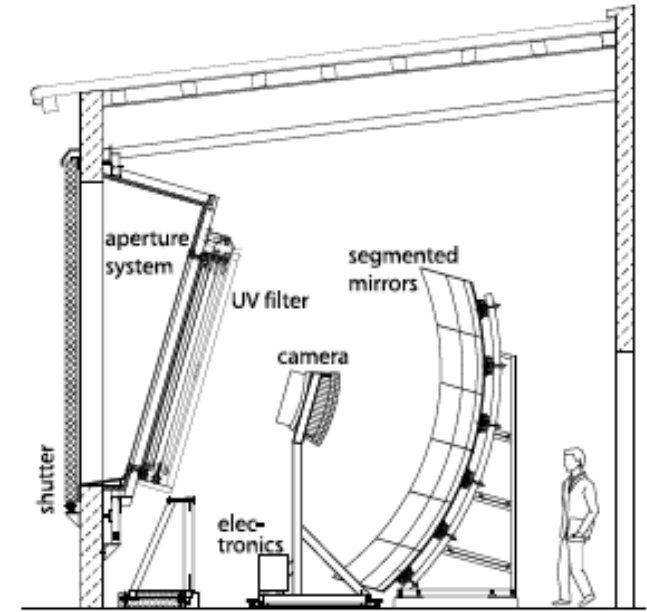
Relic neutrino is captured by beta-unstable material such as tritium:
 $\nu_e + {}^3H \rightarrow {}^3He + e^-$,
 then search for electrons with energies above the endpoint of tritium beta decay.



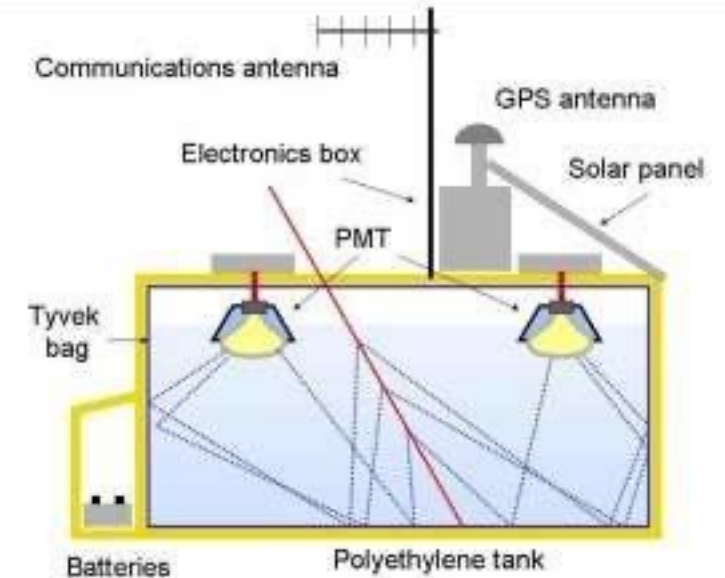
Muon Detectors

Muon detection can be applied to:

- ***extensive air showers that produce muons***
 - fluorescence in atmospheric nitrogen, water Cherenkov, or scintillation from muon decay products [Pierre Auger experiment]

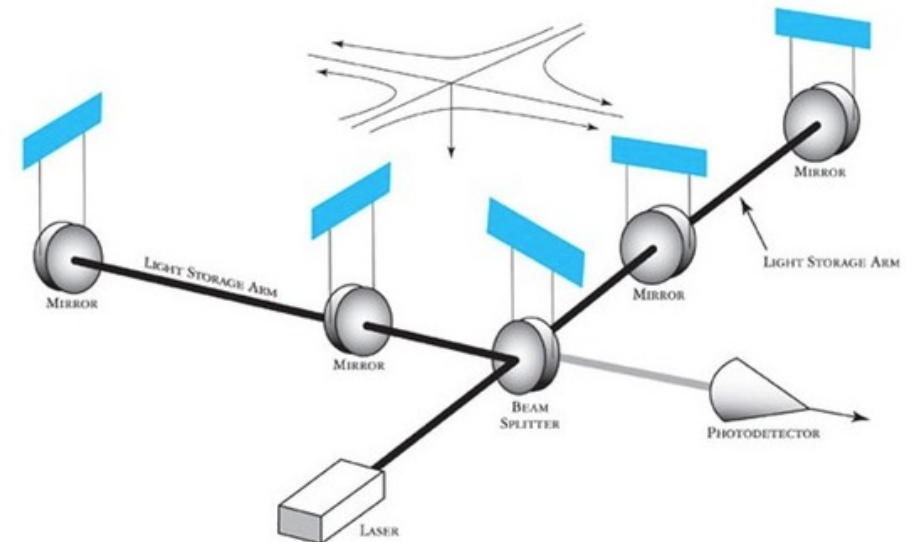
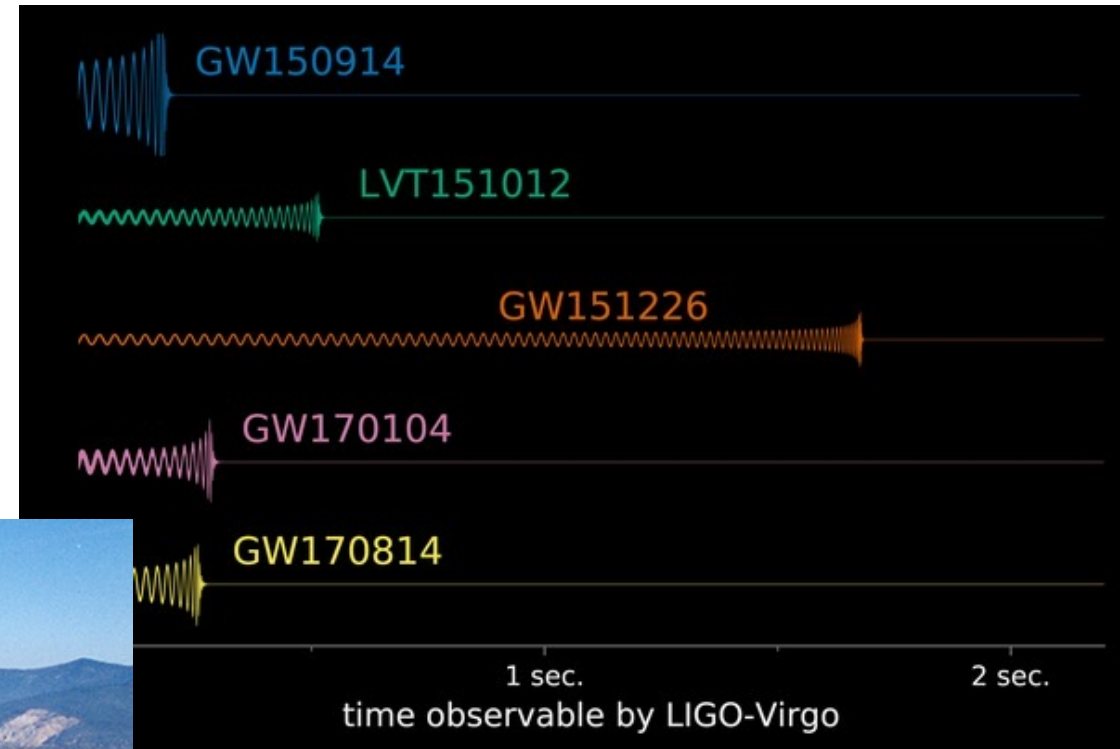


- ***detectors at accelerators such as the LHC***
 - tracking detectors in a magnetic field, to sense momentum:
 - proportional chambers (LHCb),
 - GEMs (LHCb),
 - cathode strip chambers (MSGCs, ATLAS and CMS)
 - monitored drift tubes (ATLAS, CMS)
 - To form triggers based on muons:
 - a very fast Resistive Plate Chamber (RPC). This is 2 parallel plates (anode and cathode) of high resistivity plastic, separated by a gas volume. Traversing muon scatters electrons from the gas; electrons are picked up by external metallic strips.
 - and Thin Gap Chambers (TGC), ATLAS.



Marvelous detectors not yet mentioned –

Gravitational wave detectors based on interferometry [LIGO, VIRGO].



Looking to the future....some breakthrough ideas under intense development

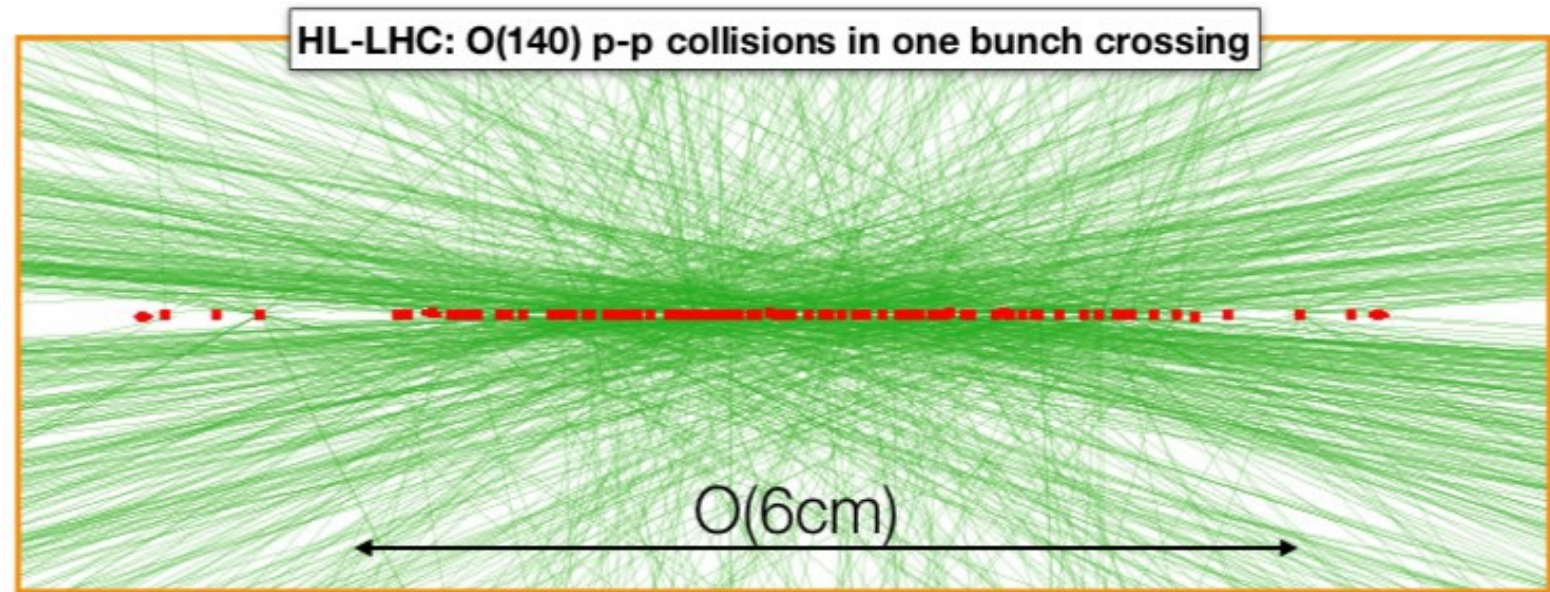
- *Precision timing detectors for particle tracking*

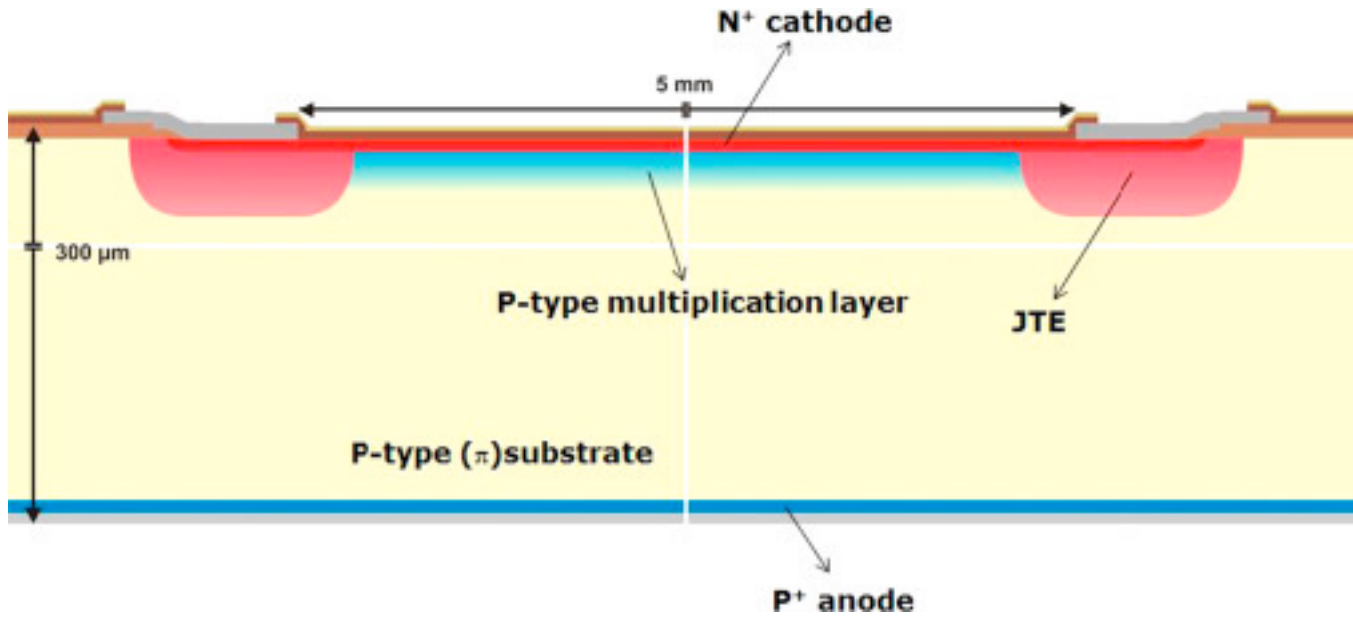
Application to extreme track densities in high luminosity particle colliders, where for example at the HL-LHC there will be 140-200 pp collisions per bunch crossing (1.6 interactions per millimeter). Goal: 30 ps resolution.

Examples:

- Low Gain Avalanche Detectors (LGADs)
- 3D Silicon Sensors for speed and gain

(images on next slide)





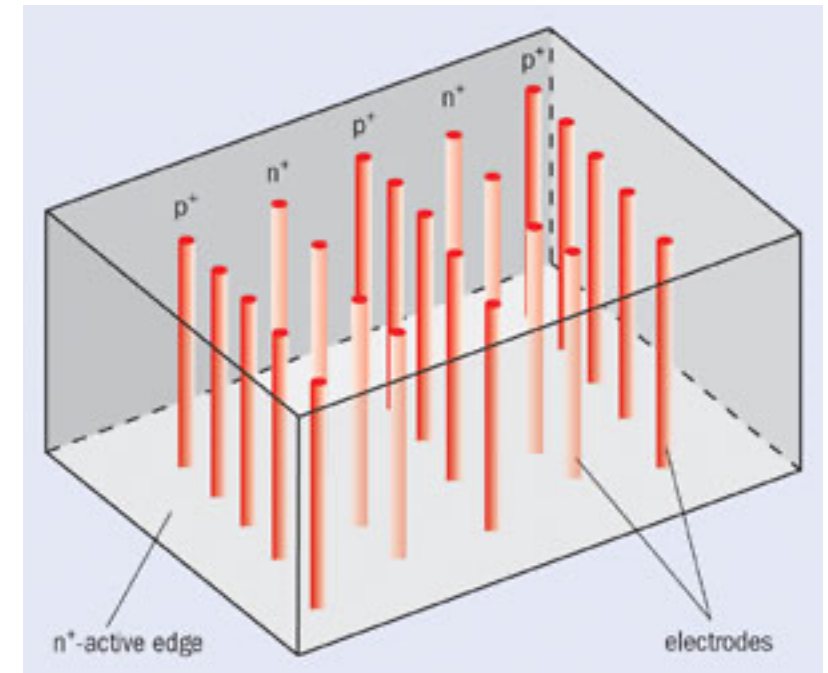
3D Silicon sensor: Electrodes are perpendicular to the wafer surface.

Very small inter-electrode separations may provide signal multiplication and time resolutions of ~few picoseconds.

LGAD: A planar p-type silicon sensor with a p-layer diffused below the cathode.

Under reverse bias, this $n^+/p/p^-$ junction produces a localized high E field region which multiplies electrons reaching the n^+ electrode.

Gain is limited to 10. Goal is timing resolution of 30 ps. Presently tolerant to $\sim 10^{15} n_{eq}/cm^2$ fluence.



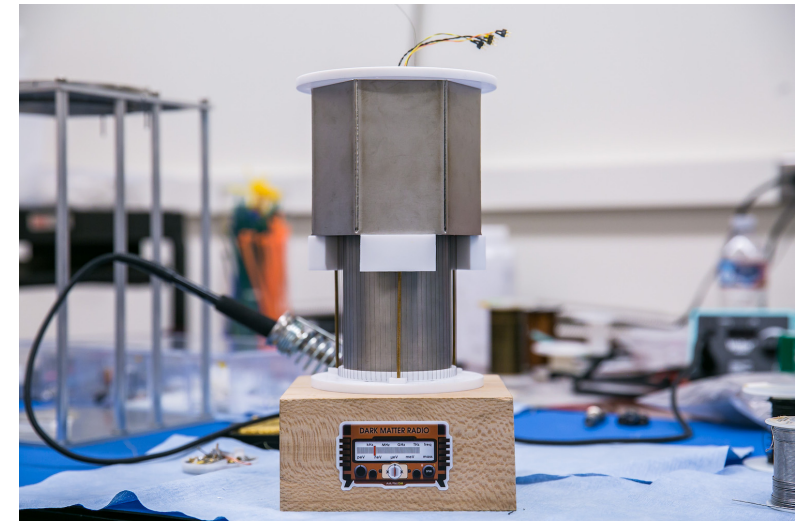
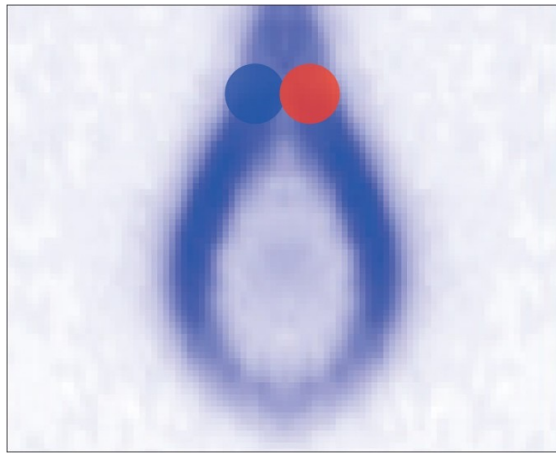
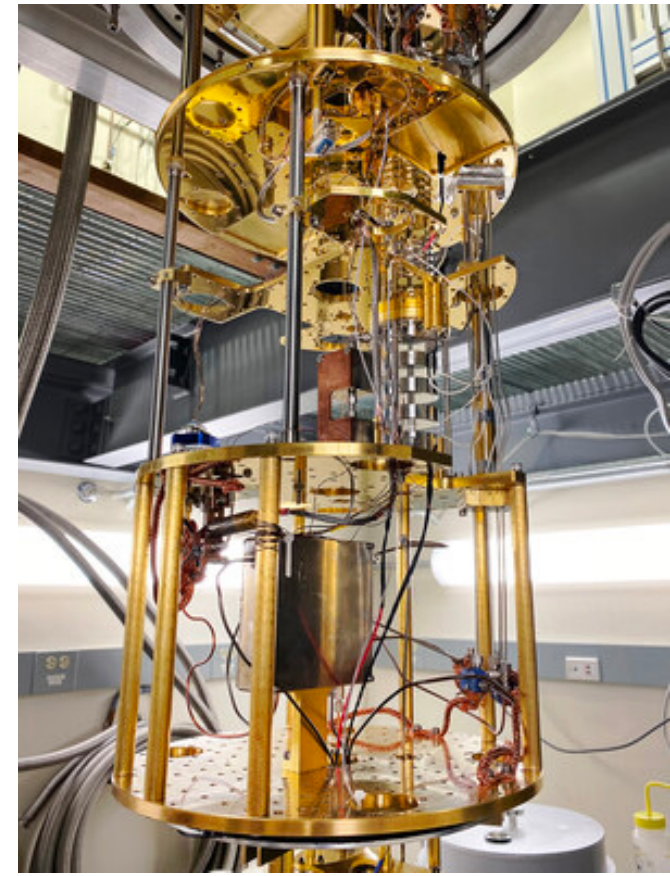
More breakthrough ideas under intense development

- *Quantum sensors*

Search for New Physics through observation of electromagnetic fields induced by QCD axions or dark photons in a cryogenic microwave cavity, using quantum squeezing to reach beyond the Standard Quantum Limit.

Examples:

- HAYSTAC experiment searches for axionic cold dark matter
- Microwave SQUIDs for the Dark Matter Radio experiment
- Dirac semimetals' tunable bandgap for low thermal noise dark matter search

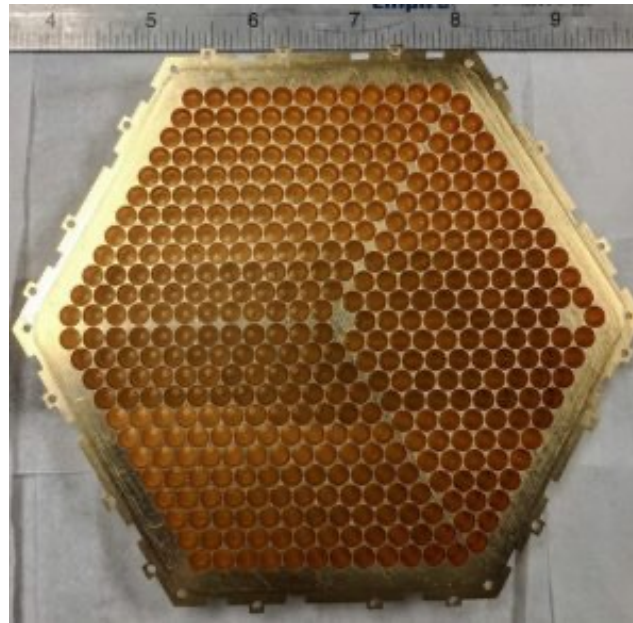
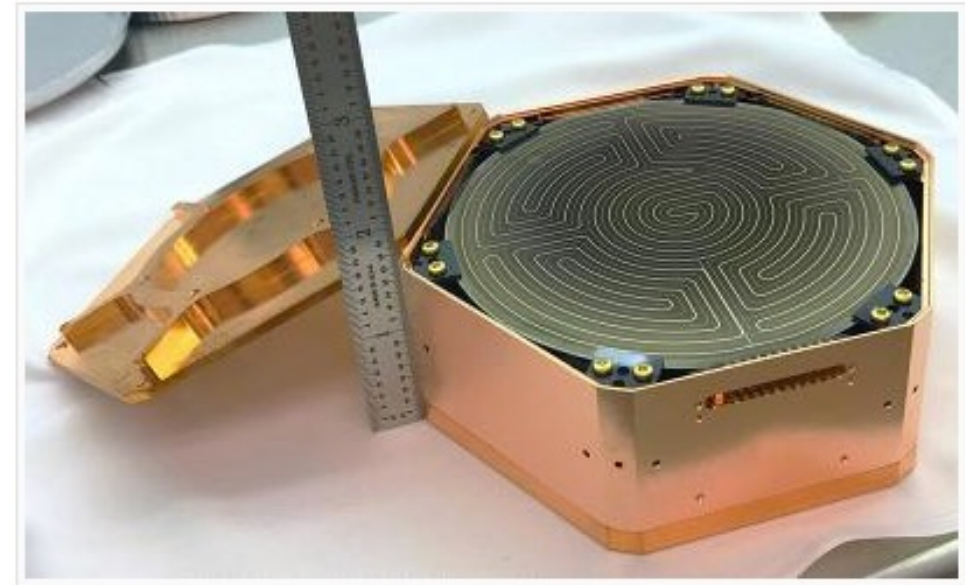


More breakthrough ideas under intense development

- *Transition edge detectors*

Ultra-sensitive thermometers: a thin superconducting film weakly heat-sunk to a bath temperature below superconductor T_c . Thermal fluctuations are highly suppressed.

Applied to dark matter (CDMS, SuperCDMS) and Cosmic Microwave Background (CMB-S4) studies



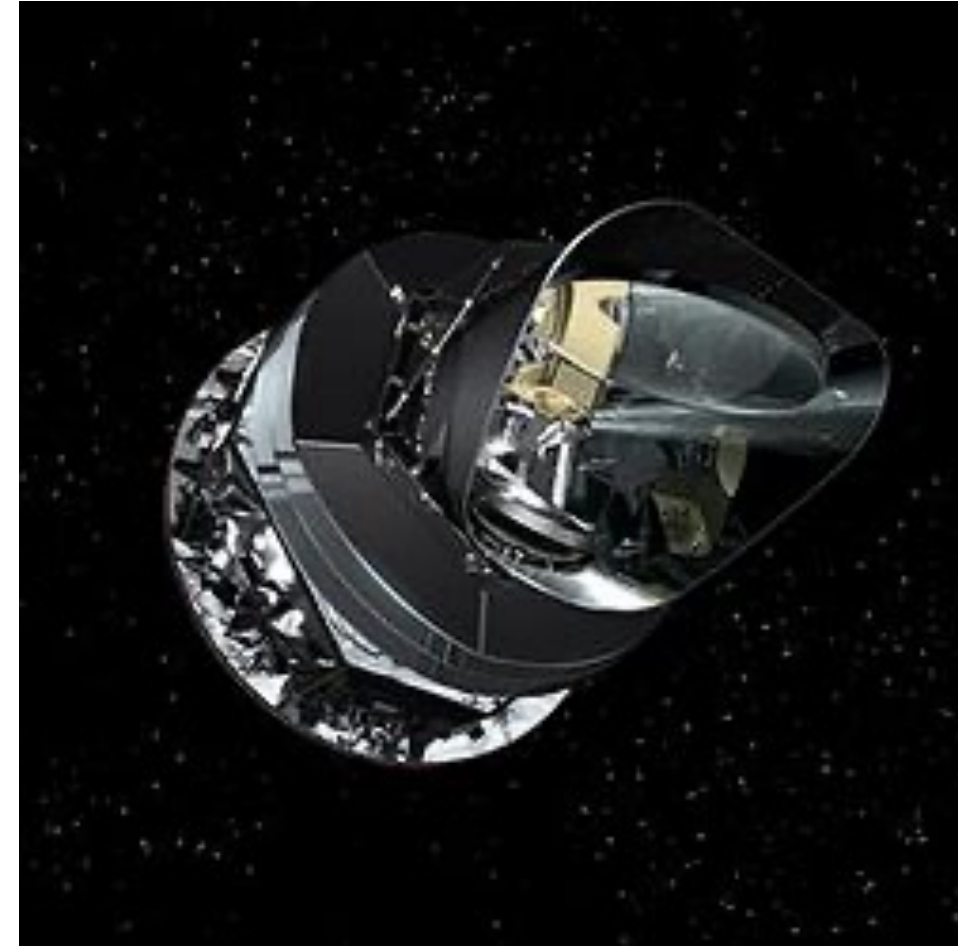
More breakthrough ideas under intense development

- *Kinetic inductance detectors*

Photons incident on a strip of superconducting material break Cooper pairs and create excess quasiparticles – this causes the kinetic inductance of the strip to rise.

When combined with a capacitor to form a microwave resonator, this detector senses the absorption of photons through change to the resonant frequency.

This superconducting technology could be applied to CMB, dark matter, and primordial density fluctuation measurements using the Planck instrument.



In conclusion...

Inventing and developing instrumentation for particle physics applications is an intensely creative endeavor.

Frequently the instruments themselves open up completely new vistas for exploration.

Please, join the community. You are welcome.